Medical University "Prof. D-r Paraskev Stoyanov" - Varna
Faculty of Medicine
Department of Anatomy and cell biology

Scientific supervisor: Prof. D-r Irina Stoyanova – van der Laan MD, PHD

Iskren Boyanov Velikov

Role of transcription factor Zbtb20 in cerebellar development

ABSTRACT
Of a dissertation for the award of the educational and scientific degree "Philosophy Doctor (PHD)"

Scientific field: Medicine, code 07.01.00

Scientific specialty
"Anatomy, Histology and Cytology"
code: 03.01.02

Varna
2025

The doctoral student works as an assistant at the Department of "Anatomy and Cell Biology" at the Medical University "Prof. Dr. Paraskev Stoyanov - Varna". The experimental work on this work was carried out under the supervision of Prof. Dr. Irina Stoyanova - van der Laan D.M., PHD at the Medical University "Prof. Dr. Paraskev Stoyanov - Varna". The dissertation field is of the specialty "Anatomy, Histology and Cytology" - code 03.01.02. It is presented on 140 pages and is illustrated with 97 figures. 254 references are cited. The dissertation was discussed at a meeting of the Department Council of the Department of Anatomy and Cell Biology at the Medical University - Varna on 26th of March and is directed for a public presentation before a scientific jury.

The public presentation of the Dissertation will take place on 25th of June from .... h. through a videoconference.

Composition of the scientific jury:

External members:

1. Prof. Dr. Stefan Todorov Sivkov, PhD
2. Prof. Dr. Iveta Antonova Koeva, PhD
3. Prof. Dimitrinka Yordanova Atanasova-Dimitrova, PhD

Reserve external member:

Prof. Dr. Nikolay Dimitrov Dimitrov, PhD

Internal members:

1. Assoc. Prof. Dr. Stoyan Pavlov Pavlov, PhD
2. Assoc. Prof. Dr. Meglena Valdemarova Angelova, PhD

Reserve internal member:

Prof. Dr. Anton Bozhidarov Tonchev, PhD, Dsc

CONTENTS

ABBREVIATIONS:

aCasp3 – activated caspase 3
Barhl1 – BarH – like Homeobox1
BG – Bergmann glia
BrdU - bromodeoxyuridine
DCN – deep cerebellar nuclei
DCX – Doublecortin
EGL – external granular layer
GABA – gamma-aminobutyric acid
GCPs – precursors of granular neurons
GCs – granular neurons
GFAP – glial fibrillary acidic protein
IGL – internal granular layer
ML – molecular layer
Pax2 – Paired box protein Pax2
Pax6 – Paired box protein Pax6
PBS – phosphate buffer
RL – rhombic lip
RMS – rostral migratory stream
SGZ – subgranular zone
UBC – unipolar brush cells
VZ – ventricular zone
WM – white matter
Zbtb20 - zinc finger and BTB-domain containing 20
DNA – deoxyribonucleic acid
RNA – ribonucleic acid
CNS – central nervous system

1. Introduction

The nervous system is a set of structures that carry out the integration and adaptation of the organism. According to the topographic principle, it is divided into central and peripheral. The main tissue that builds the structures of the nervous system is nervous tissue. It is composed of two cellular components: nerve cells (neurons) and neuroglia. The main structural and functional unit is the neuron. This term was first introduced by Waldeyer in 1891.

The nervous system develops from the neural tube. From its anterior expanded part (the rudiment of the cerebrum) through two pinchings, three primary brain vesicles are formed: anterior - prosencephalon, middle - mesencephalon, and posterior - rhombencephalon. Later, the anterior vesicle is divided into two parts - telencephalon and diencephalon. The hindbrain is divided into: metencephalon and medulla oblongata. The hindbrain gives rise to the pons and the cerebellum. The organogenesis of the nervous system is also accompanied by the histogenesis of the nerve elements. The process of formation of new functionally active neurons from stem or progenitor cells is called neurogenesis.

The cerebellum has three main functions: maintaining the equilibrium position of the body in space, maintaining muscle tone and coordinating voluntary movements. Two lateral parts are distinguished in the cerebellum: cerebellar hemispheres - hemispheria cerebelli and a small, underdeveloped part located between them - vermis. The surface of the cerebellum is furrowed by deep fissures - fissurae cerebelli, which separate the cerebellar leaves - folia cerebelli. Phylogenetically and functionally, the cerebellum is divided into anterior, posterior and flocculonodular lobes. It is also subdivided into three parts: old - paleocerebellum, ancient - archicerebellum, new - neocerebellum. In each of these areas, different molecular mechanisms of gene expression operate, which leads to functional differences (Chen, Hanson et al. 1996; Sillitoe and Joyner 2007). Using Larsell's criteria for the vermis, the cerebellum of all mammals can be divided into ten main lobes. Each of these is further subdivided into secondary and tertiary sublobes (Larsell 1970). The cerebellum is made up of: cortex (cortex cerebelli), centrally located white matter - corpus medullare and nuclei lying in the white matter. The cerebellar cortex is histologically homogeneous and divided into three clearly distinguishable cell layers - molecular layer, Purkinje cell layer and granular layer. These layers lie over a core of white matter and the cerebellar nuclei (DCN). White matter is made up of bundles of axons, forming input and output pathways.

Modern molecular, genetic, physiological and anatomical methods are constantly evolving. However, many processes related to neurogenesis, neuronal migration and synapse formation

in the developing brain remain unclear. Establishing the mechanisms of embryonic brain development is a challenge for modern neuroscience. Disturbances in these mechanisms at the gene level lead to brain damage. Their clarification will contribute to the improvement of therapeutic approaches in clinical neuroscience. The present study aims to shed more light on the role of transcription factors, and in particular Zbtb20, in the development of the cerebellum.

2. Hypotheses of the Dissertation

1. The transcription factor Zbtb20 affects the cerebellar development in mice.
2. The transcription factor Zbtb20 does not affect the cerebellar development in mice.

3. Aim and tasks of the study:

In conducting our study, we set ourselves the following goals:

1. To establish the role of the transcription factor Zbtb20 in the development of neuronal and neuroglial cell populations.
2. To establish the role of Zbtb20 in the process of cerebellar foliation.

We set ourselves the following tasks:
1. To explore the normal expression of Zbtb20 in the cerebellum of wild-type mice at different age periods (E16 and P30).
2. To measure the area of the different layers – external granular, molecular, internal granular, Purkinje layer at the three age periods – P4, P8 and P12 in wild-type individuals and mutants.
3. To establish the cell population of astrocytes and Bergmann glia at P4, P8 and P12 in controls and mutants, using GFAP- antibody.
4. To establish the cell population of Purkinje cells at P4, P8 and P12 in controls and mutants using Calbindin- antibody.
5. To perform a quantitative and qualitative analysis of Neun+ cells at P4, P8 and P12 in controls and mutants.
6. To perform a quantitative and qualitative analysis of Calretinin+ cells at P4, P8 and P12 in controls and mutants.

7. To monitor the proliferative potential of the cells of the developing cerebellum using the marker Ki-67.
8. To perform a quantitative and qualitative analysis of Tbr2+ cells at P4, P8 and P12 in controls and mutants.
9. To perform a quantitative and qualitative analysis of Zbtb20+ cells at P4, P8 and P12 in controls and mutants.

4. Material and methods

Experimental animals and tissue preparation:

For the purpose of our study, Zbtb20 mutant mice were used. The studies were performed in accordance with the German Animal Protection Act, after approval of the experiments by the Niedersächsische Landesamt für Verbraucherschutz und Lebesmittelsicherheit (LAVES) / Oldenburg, contract no. 33.9-42502-04-11 / 0622 dated 07.12.2011. The experiments were completed before January 1, 2013. Homozygous mice were generated by crossing heterozygous animals, which allows a direct comparison of gene expression patterns between homozygous controls (+/+), heterozygous mutants (+/-) and homozygous mutants (-/-). For the analysis, the mice were killed by cervical dislocation or by CO_2 inhalation. Knockout (KO) Zbtb20 mice lack the functionally important BTB/POZ domain of the protein, as well as the first of the five zinc fingers, which are replaced by a lacZ-neomycin cassette.

Wild-type mice were also used on embryonic day sixteen and postnatal day thirty. These experimental animals were provided in collaboration with the Institute of Microbiology of the Bulgarian Academy of Sciences. The protocol is No. 392 of 21. 04. 2024.

Bacteria:

Several strains of E. coli were used.

Standard solutions:

Phosphate-buffered saline (PBS); Paraformaldehyde (PFA); Tris EDTA (TE).

Isolation of plasmid DNA from E. coli cells:

Plasmid DNA (10-20 μm) was isolated from 2 ml bacterial cultures using a Miniprep kit (Qiagen) or by the alkaline lysis method.

Generation of Zbtb20 (-/-) mutants by recombination:

To generate Zbtb20-deficient mice, a vector was created using a method called recombination (recombination mediated by genetic engineering).

Preparation of cerebellar sections:

A total of 36 experimental animals were used. Of these, 6- Zbtb20-/- and 6- Zbtb20+/+ on P4; 6- Zbtb20-/- and 6- Zbtb20+/+ on P8; 6- Zbtb20-/- and 6- Zbtb20+/+ on P12. Labeling with the nucleotide analogue bromodeoxyuridine (BrdU) was done by intraperitoneal injection on E10; E12.5; E14.5, respectively. The dosage was 40 mg/kg. After sacrifice of the experimental animals, the brain was removed from the cranial cavity and the cerebellum was separated from the rest of the brain. The tissue was then placed in cold Krebs buffer. The tissue blocks were embedded in 4% agarose solution. They were then placed in 4% paraformaldehyde solution for fixation for 1 hour. The fixed tissue was then rinsed with PBS, embedded in sucrose solution and subsequently frozen. Cryostat sections - 10 μm thick were made. Antigen retrieval was performed by heating in a microwave oven (800 W, 3 times, 5 minutes each) in citrate buffer (pH 6.0). The sections were then washed and blocked for 1 hour in blocking solution containing normal serum. Primary antibodies were incubated overnight at 4°C in the blocking solution. After washing, the sections were incubated with species-specific secondary antibodies from the Alexa series (Invitrogen) in blocking solution for 2 h at room temperature (RT), washed again and mounted with Vectashield mounting medium (Vector Labs) containing DAPI.

Immunofluorescence:

After rinsing in PBS solution, the tissue sections were placed in sodium citrate solution, pH 6.0 for antigen retrieval. Incubation was performed with primary antibodies, followed by secondary antibodies. Staining was followed by 4`,6`- diamino-2- phenylindole (DAPI).

Primary and secondary antibodies:

We used the following primary antibodies and the corresponding dilutions: Rabbit monoclonal antibodies: anti- calbindin (1:500) from Sigma; anti- calretinin (1:400) from Chemicon; anti- Ki-67 (1:100) from Lab Vision (thermoscientific); anti- Pax2 (1:100) from Invitrogen; anti-caspase-3 (1:200) from Santa Cruz; anti-Ki67 (1:100) from Dako; anti-NeuN (1:100) from Millipore; anti-Pax6 (1:300) from Covance; anti-Pax6 (1:100) from Invitrogen; anti-Tbr1 (1:300) from Abcam); anti-Tbr2 (1:200) from Chemicon. Goat monoclonal antibodies: anti- doublecortin (1:500) from Santa Cruz. Chicken monoclonal antibodies: anti-GFAP (1:400) from Thermo Scientific. Secondary antibodies (Alexa series; 1:200) from Invitrogen.

Microscopy and statistical processing:

The observation of the images and their photography was carried out using a fluorescent microscope “Zeiss” at the Department of “Anatomy and Cell Biology” of the Medical University of Varna. Objectives with magnifications: x5, x10, x20, x40 were used. The processing of the images, the measurement of the areas and the counting of cells was carried out using the software product Image J (Fiji). We used the ROI function. The statistical processing of the data was carried out using the Microsoft Excel program. The statistical differences between the studied groups were established using the functions: standard deviation (ST Dev), as well as Student's T-test. We consider the difference between controls and mutants to be statistically significant if in the T-test - $p < 0.05$.

Results

To explore the normal expression of Zbtb20 in the cerebellum, we performed immunofluorescence staining with Zbtb20 on embryonic day sixteen (E16) in control mice. We found expression in the region of the cerebellar primordium – the rhombic lip (RL). This is also a progenitor zone for neurons and glia (Fig. 1).

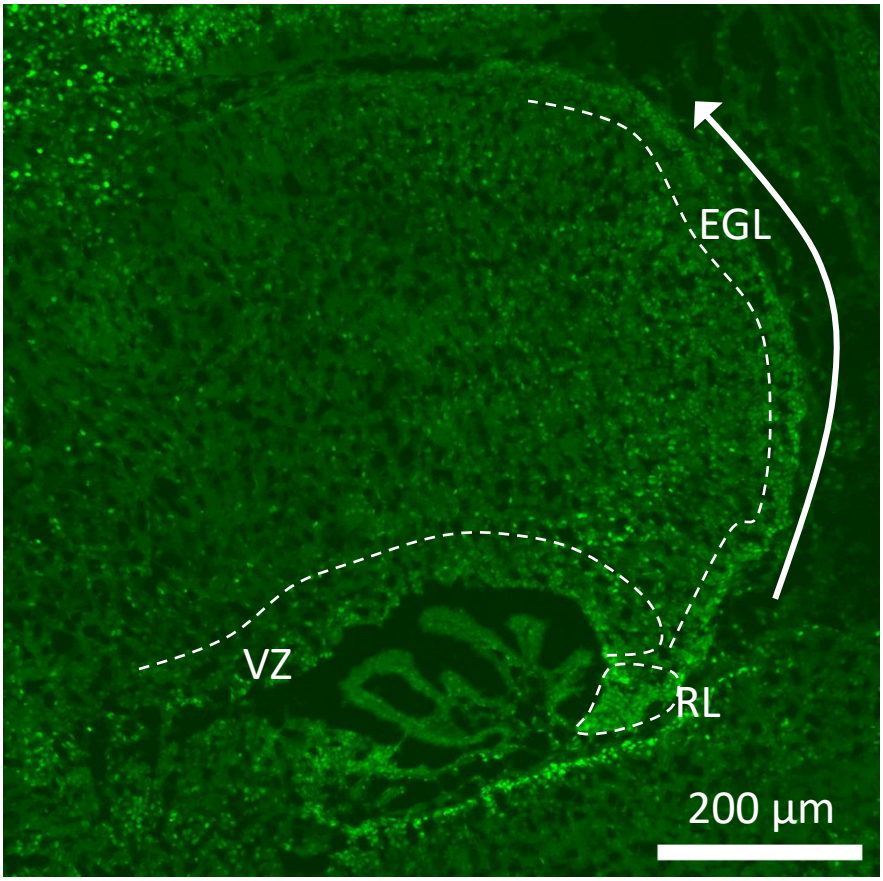

Fig. 1 – The rhombic lip (RL) is shown, where the cerebellar rudiment is located. We also observe the ventricular zone (VZ) and the external granular layer (EGL). Magnification x5. The photo is presented with the consent of Dr. Dimo Stoyanov, MD and Dr. Lora Veleva.

On the sixteenth embryonic day, we explored the expression of the Zbtb20 and Pax6 markers. We examined four areas of the developing brain in wild-type mice. These are: external rhombic lip (ERL), internal rhombic lip (IRL), external granular layer (EGL) and Purkinje cell plate (PCP). In the external rhombic lip, we found 98 Zbtb20-immunoreactive cells. Of these, 28 are also immunoreactive for the Pax6 marker, i.e. 29.08% double-positive cells (Zbtb20+/Pax6+) of all Zbtb20+ cells. In the same area, we found 114 Pax6+ cells. Of these, 28 are also immunoreactive for the Zbtb20 marker, i.e. 24.89% double-positive cells (Zbtb20+/Pax6+) of all Pax6+ cells. In the inner rhombic lip, we found 77 Zbtb20 – immunoreactive cells. Of these, 17 are also immunoreactive for the Pax6 marker, i.e. 22.6% double-positive cells (Zbtb20+/Pax6+) of all Zbtb20+ cells. In the same area, we found 70 Pax6+ cells. Of these, 17 are also immunoreactive for the Zbtb20 marker, i.e. 25% double-positive cells (Zbtb20+/Pax6+) of all Pax6+ cells. In the outer granular layer, we found 166 Zbtb20-immunoreactive cells. Of these, 22 are also immunoreactive for the Pax6 marker, i.e. 13.51%

double-positive cells (Zbtb20+/Pax6+) of all Zbtb20+ cells. In the same zone, we found 126 Pax6+ cells. Of these, 22 are also immunoreactive for the Zbtb20 marker, i.e. 17.79% double-positive cells (Zbtb20+/Pax6+) of all Pax6+ cells. In the Purkinje cell plate, we found 165 Zbtb20-immunoreactive cells. Of these, 6 are also immunoreactive for the Pax6 marker, i.e. 3.63% double-positive cells (Zbtb20+/Pax6+) of all Zbtb20+ cells. In the same zone, we found 187 Pax6+ cells. Of these, 6 were also immunoreactive for the Zbtb20 marker, i.e. 3.2% double-positive cells (Zbtb20+/Pax6+) out of all Pax6+ cells (Fig. 2).

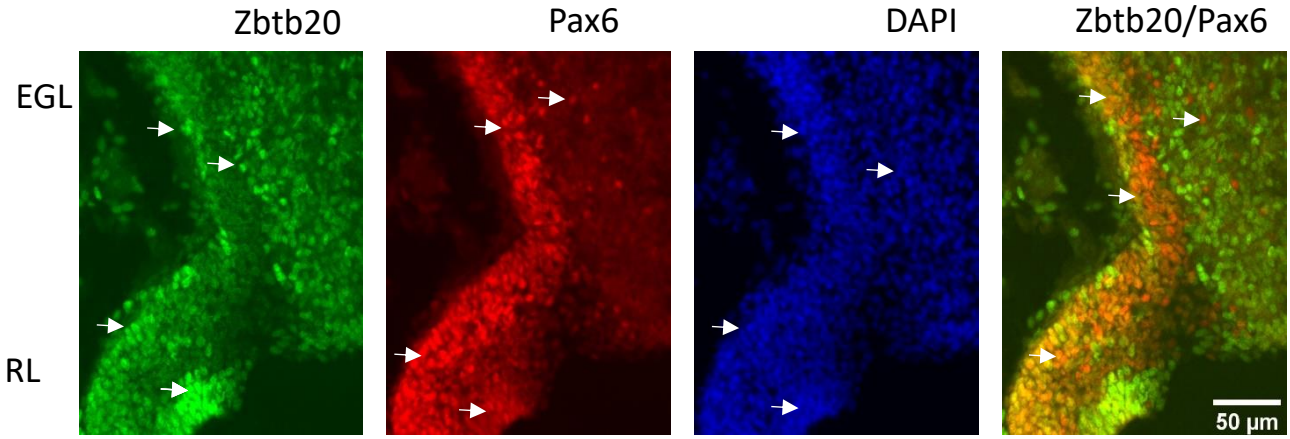

Fig. 2 – Fluorescence micrographs showing the expression of Zbtb20 and Pax6 (arrows) in the rhombic lip and the outer granular layer of E16: A) and B) illustrate the expression of only Zbtb20 and Pax6, respectively; C) selective labeling of the nuclei with DAPI, which allows to determine the total number of cells in the studied area; D) the image is obtained by superimposing A and B, as a result of which the double-labeled cells are stained in orange (arrows). Magnification x10. The photo is presented with the consent of Dr. Dimo Stoyanov and Dr. Lora Veleva.

To determine the colocalization of Zbtb20+ and Neun+ cells, we examined the cerebellum of adult wild-type individuals at postnatal day thirty (P30). We also applied DAPI staining. We do not detect double-positive neurons (Neun+ and Zbtb20+) in the cerebellar cortex. This means that in adult individuals, neurons do not express Zbtb20 (Fig. 3).

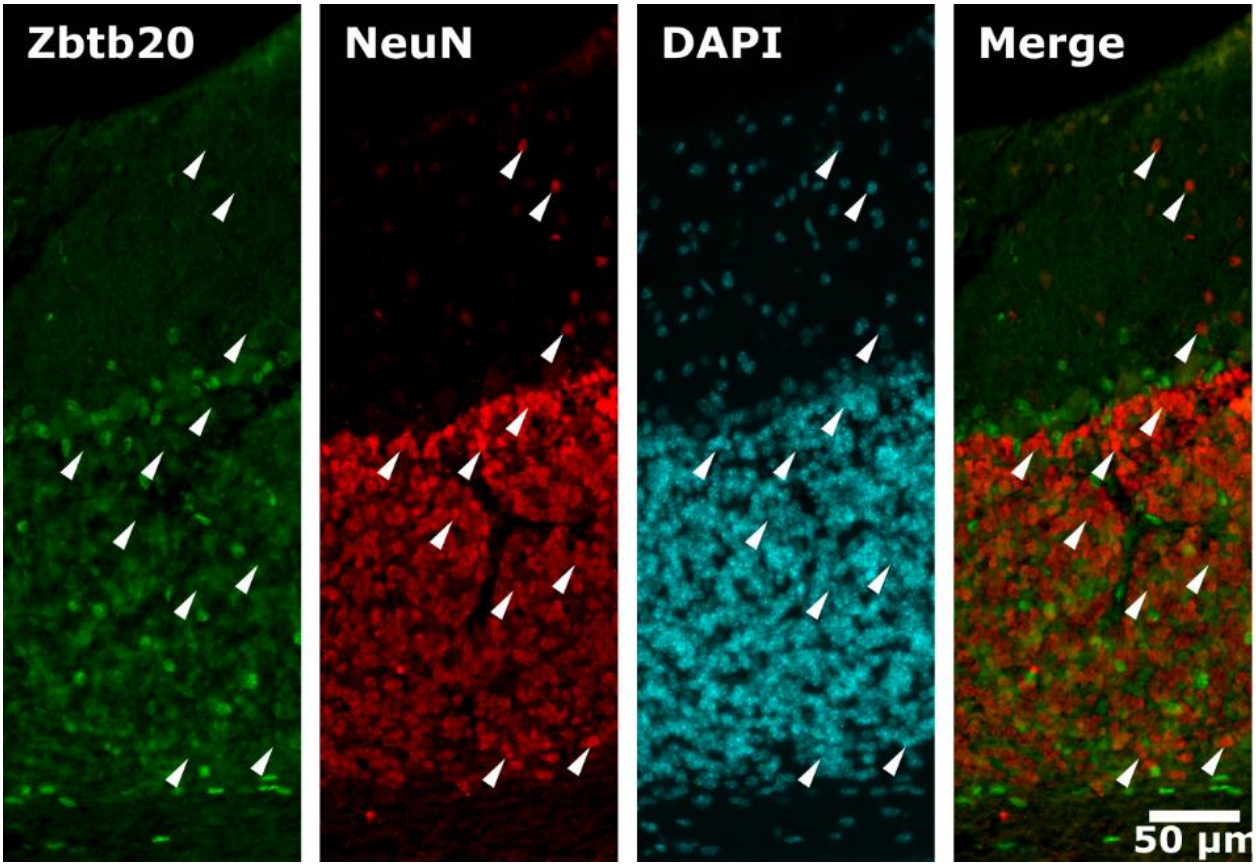

Fig. 3 - Darkfield micrograph illustrating the presence of NeuN+ cells (in red) and Zbtb20+ cells (in green). Overlaying the two images shows that there are no double-labeled neurons in the cerebellar cortex. All cell nuclei are stained with DAPI. Magnification x5. The image is provided with the consent of Dr. Dimo Stoyanov and Dr. Lora Veleva.

To determine the colocalization of Zbtb20+ and Calretinin+ cells, we examined the cerebellum of adult wild-type individuals at P30. We also applied DAPI staining. The cells that are positive for Zbtb20 are not immunopositive for Calretinin. We do not detect double positive unipolar brush cells (Zbtb20+ and Calretinin+) (Fig. 4).

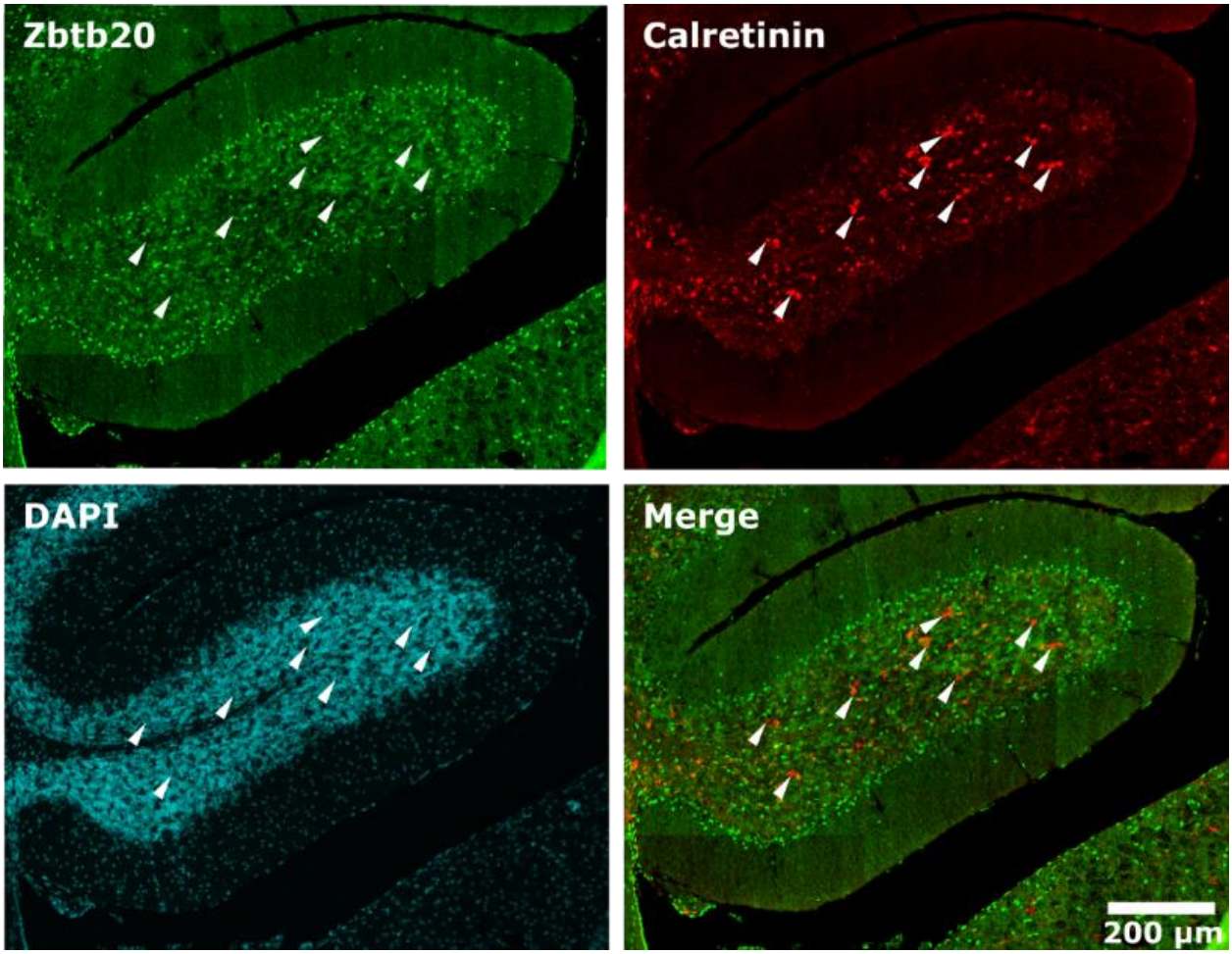

Fig. 4 - Fluorescence micrograph of cerebellar cortex from a wild-type mouse at P30. Zbtb20+ neurons are labeled in green, and unipolar brush cells, visualized with their marker Calretinin+, are represented in red. The arrows in all three images point to the same unipolar brush neurons. The superimposition of the two images (merge) visualizing the markers shows that Zbtb20 is not expressed in this neuronal population. The nuclei of all cells are stained blue with DAPI. Magnification x5. The image is presented with the consent of Dr. Dimo Stoyanov and Dr. Lora Veleva.

To detect the colocalization of Zbtb20+ and Pax2+ cells, we examined the cerebellar cortex of adult wild-type individuals at P30. We also applied DAPI staining. Cells that are positive for Zbtb20 are not immunopositive for Pax2. We do not detect double-positive Golgi cells type II (Zbtb20+ and Pax2+) (Fig. 5).

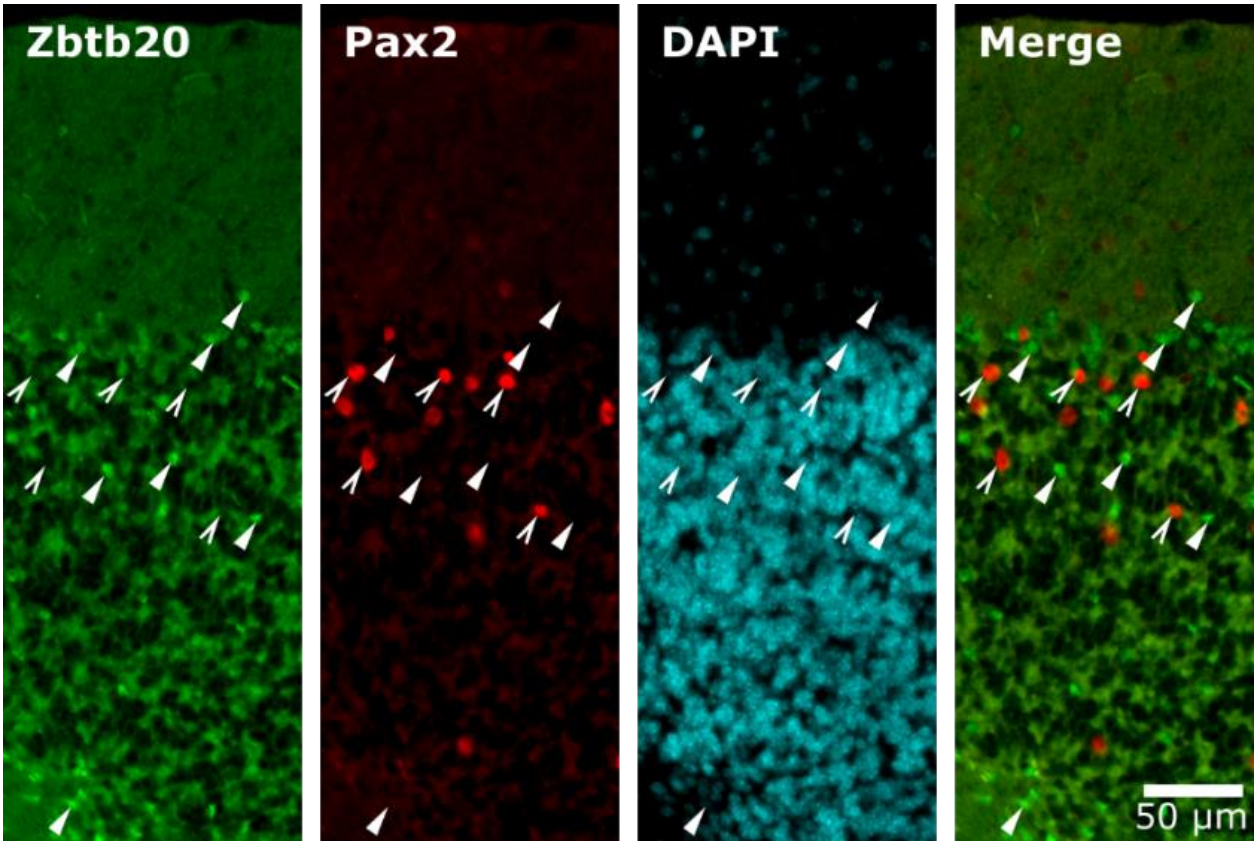

Fig. 5 - Zbtb20+ (in green, indicated by solid arrows) and Pax2+ cells (in red, indicated by open arrows) at P30. The superimposition of the two images clearly shows that there is no co-localization of the two transcriptional factors in Golgi type-2 cells (Merge). Magnification x5. The image is presented with the consent of Dr. Dimo Stoyanov and Dr. Lora Veleva.

To detect the colocalization of Zbtb20+ and Parvalbumin+ cells, we examined the cerebellum of adult wild-type individuals on P30. We also applied DAPI staining. The cells that are positive for Zbtb20 are not immunopositive for Parvalbumin. We do not detect double positive Purkinje cells (Zbtb20+ and Parvalbumin+) (Fig. 6).

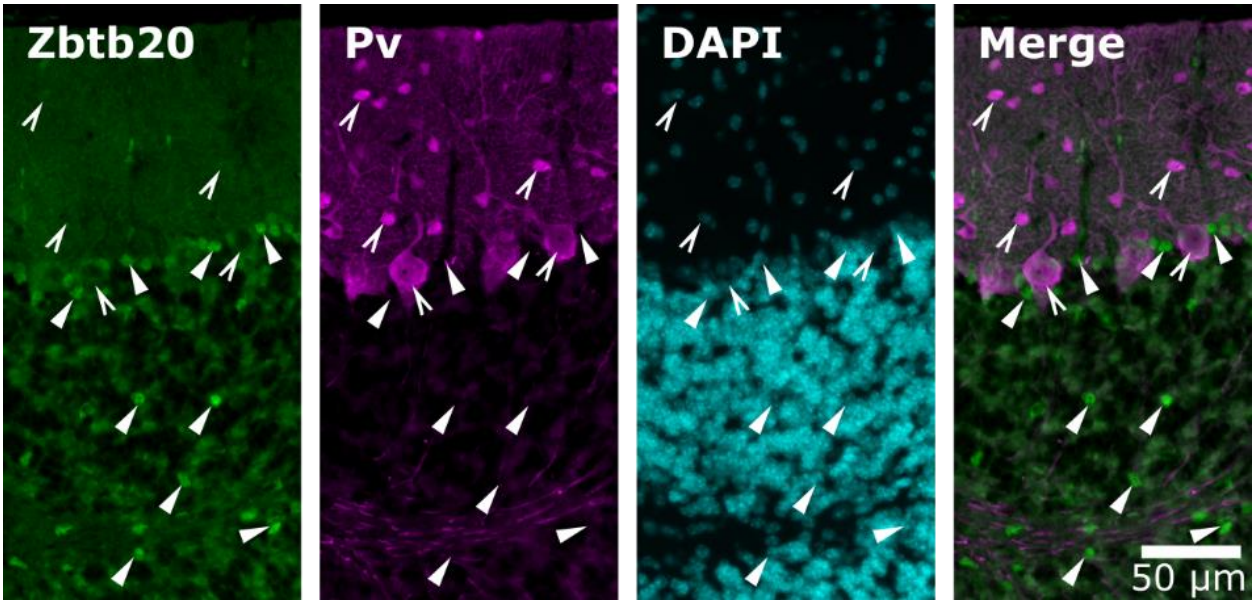

Fig. 6 - Zbtb20+ (in green, solid arrows) and Parvalbumin+ cells (in purple, open arrows), at P30. The superimposition of the two images (Merge) proves the lack of co-localization. Magnification. x5. The image is presented with the consent of Dr. Dimo Stoyanov and Dr. Lora Veleva.

To detect the colocalization of Zbtb20+ and Olig2+ cells, we examined the cerebellum of adult wild-type individuals at P30. We also applied DAPI staining. At this age, we detected oligodendrocyte (Olig2+) cells expressing Zbtb20 only in the white matter of the brain (Fig. 7).

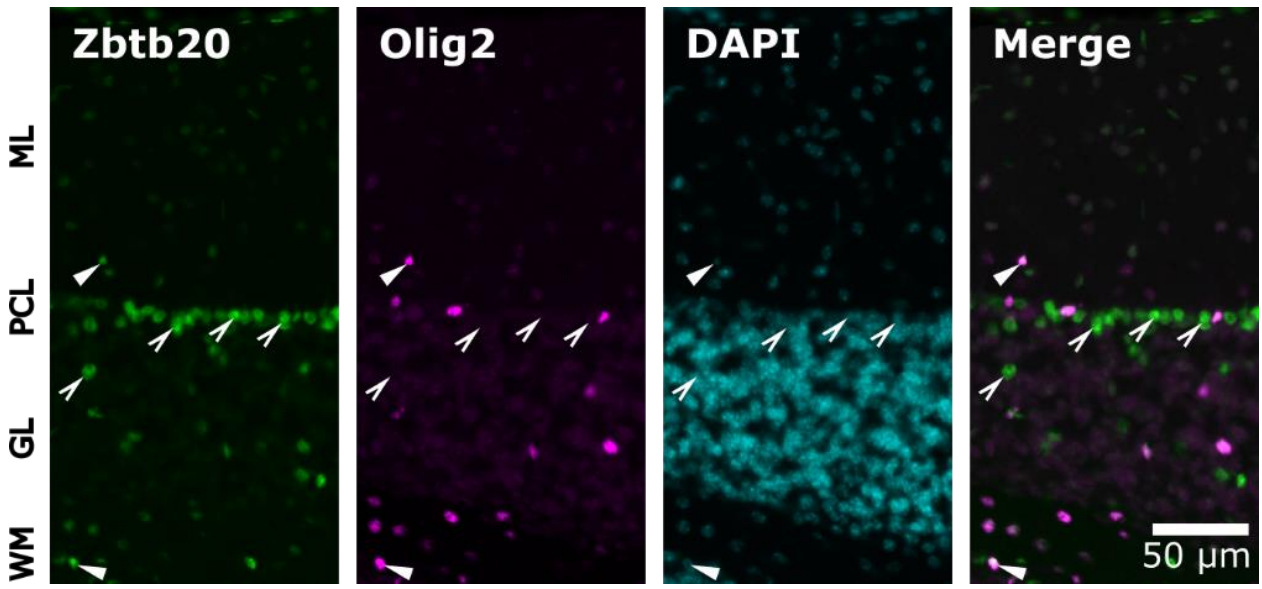

Fig. 7 - Zbtb20+ (green, open arrows) and Olig2+ cells (purple, solid arrows) at P30. From the image overlay (Merge), it is clear that co-localization is established only in the white matter (WM). GL - Golgy layer; PCL - Purkinje cell layer; ML - molecular layer. The image is presented with the consent of Dr. Dimo Stoyanov and Dr. Lora Veleva.

To determine whether Bergmann glia express Zbtb20, we examined the cerebellum of adult wild-type individuals at P30. We applied staining with the markers Blbp and DAPI. Double-positive cells (Blbp+ and Zbtb20+) are detected in the Purkinje cell layer (Fig. 8).

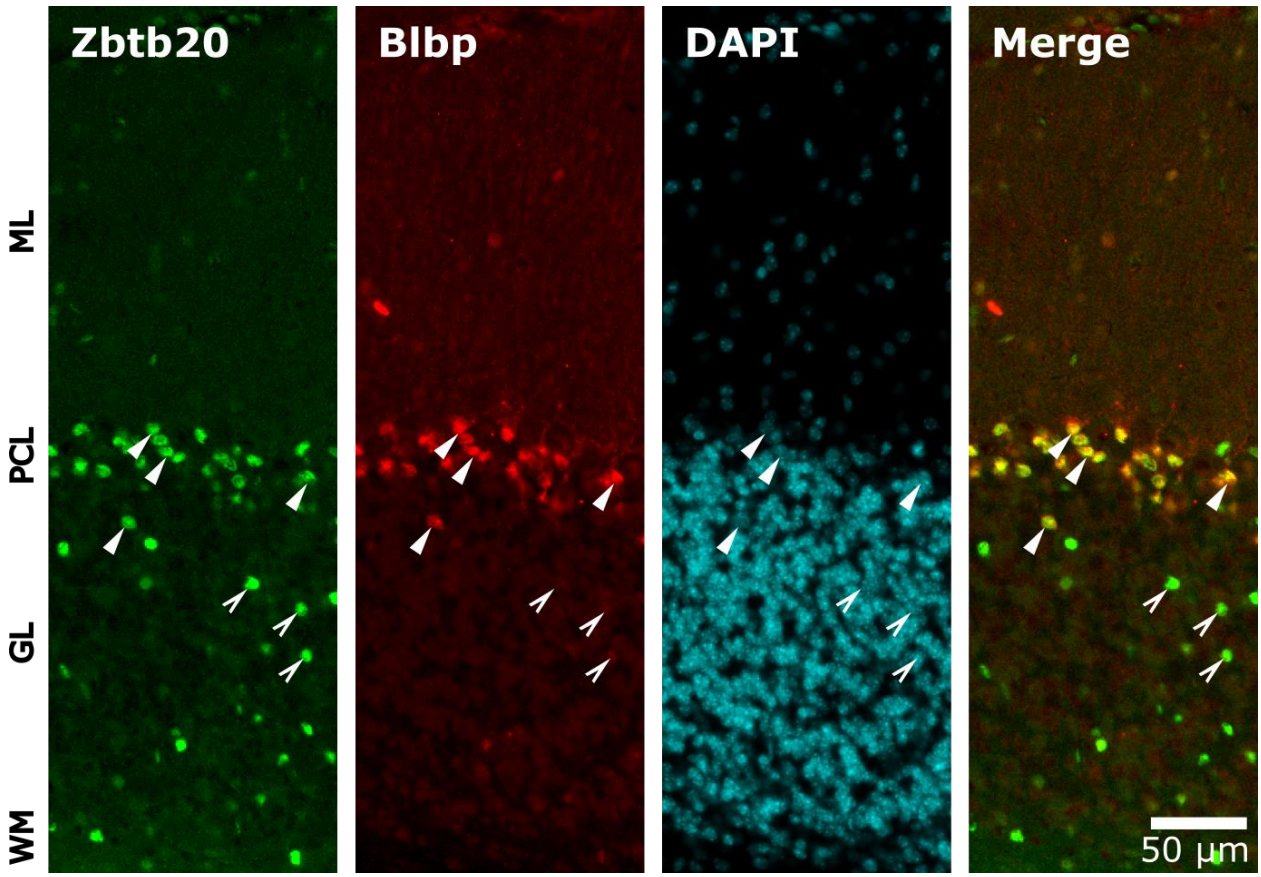

Fig. 8 - Fluorescence micrograph showing sections of cerebellar cortex positive for Zbtb20 (green, open arrows) and Blbp (red, solid arrows) at P30. Image overlay (Merge) shows that colocalization is only present in the Purkinje cell layer (yellow-orange). Image provided with the permission of Dr. Dimo Stoyanov and Dr. Lora Veleva.

To determine whether protoplasmic astrocytes in the gray matter express Zbtb20, we applied staining with the neuroglial marker GFAP at P30. We found a small number of double-positive protoplasmic astrocytes that were also positive for Zbtb20 (Fig. 9).

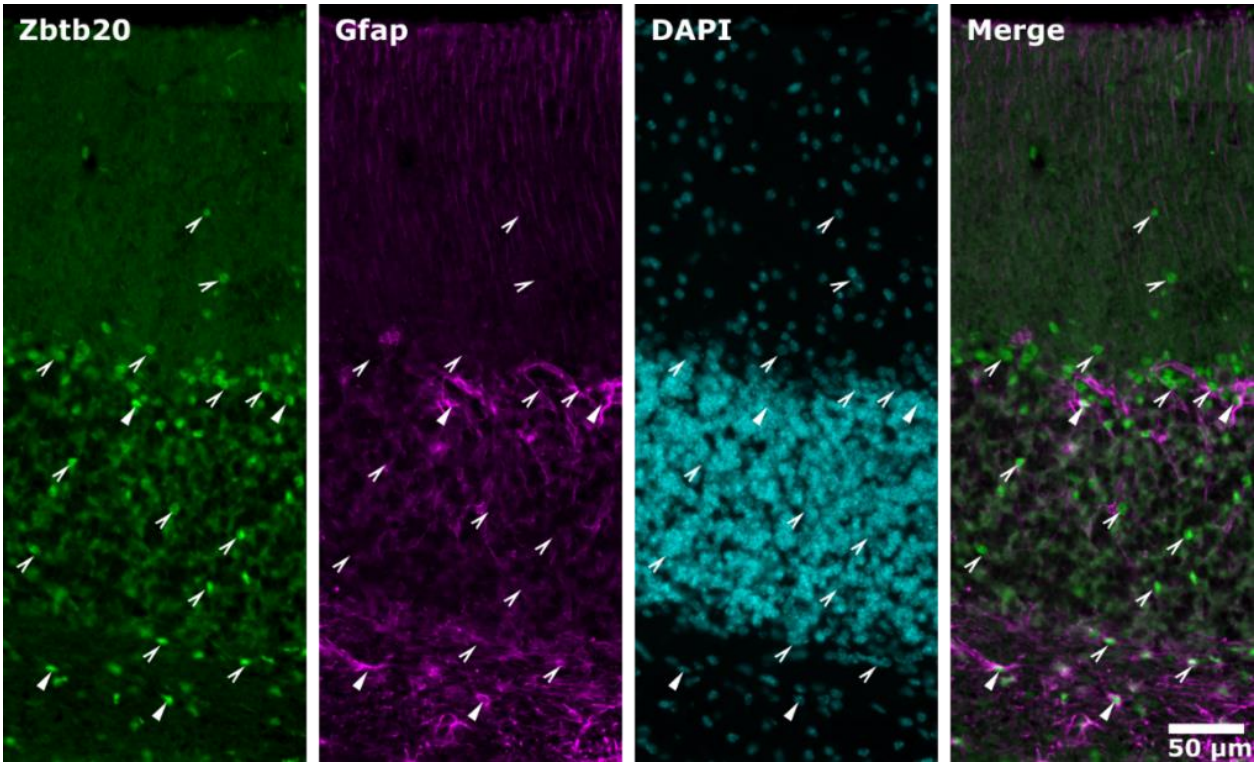

Fig. 9 – Fluorescence microscopy demonstrating the presence of GFAP- (purple, solid arrows) and Zbtb20-immunoreactivity (green cells, indicated by open arrows) in the gray matter of the cerebellum. Although in small numbers, double-labeled neuroglial cells – GFAP+/Zbtb20+ (colored almost white and indicated in the merged image by solid arrows) are observed. The image is provided with the consent of Dr. Dimo Stoyanov and Dr. Lora Veleva.

To determine whether fibrous astrocytes in the white matter express Zbtb20, we also conducted a study with the GFAP marker at age P30. We detected double-positive cells in the white matter (GFAP+ and Zbtb20+) (Fig. 10).

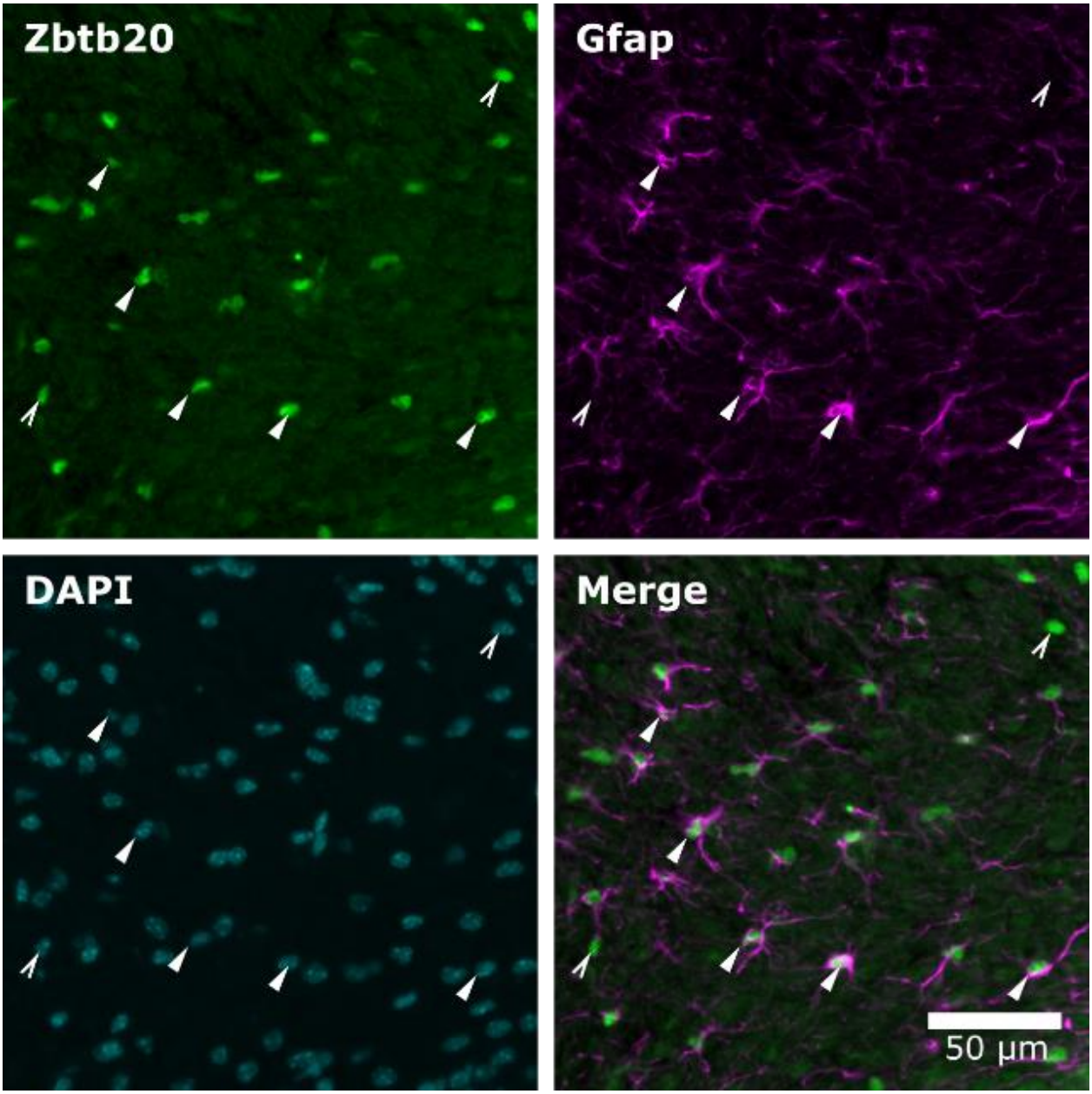

Fig. 10 – Dark-field photograph of white matter in a mouse cerebellum, demonstrating the presence of the cytoskeletal protein GFAP in the bodies and processes of fibrous astrocytes (colored purple and indicated by solid arrows). Cells positive for Zbtb20 are colored green. Overlaying the two images clearly shows the presence of Zbtb20 in the nuclei of some of the fibrous astrocytes. The photograph is provided with the consent of Dr. Dimo Stoyanov and Dr. Lora Veleva.

In order to follow the quantitative and qualitative differences in the cerebellar development in mice (wild type and mutants) we performed an immunofluorescence study with the marker DAPI (diaminophenylindole). Our interest was: the development of the cerebellar folia; the

thickness of the outer granular layer at different stages (P4, P8 and P12); the area of the outer and inner granular layers, as well as the molecular layer at different stages (P4, P8 and P12).

When studying the development of the cerebellar folia at different age periods, we found the following results: At P4, a similar number of folia was found in wild-type and mutant mice. In the region of the ninth cerebellar folia in wild-type mice, an additional cleft and subfolia were found. At stage P8, a similar number of folia were found in wild-type and mutant mice. In mutants, in the region of the third folia, as well as in the fourth and fifth folia, we found an additional cleft and an additional subfolia. At P12, a similar number of folia was found in wild-type and mutant mice (Fig. 11).

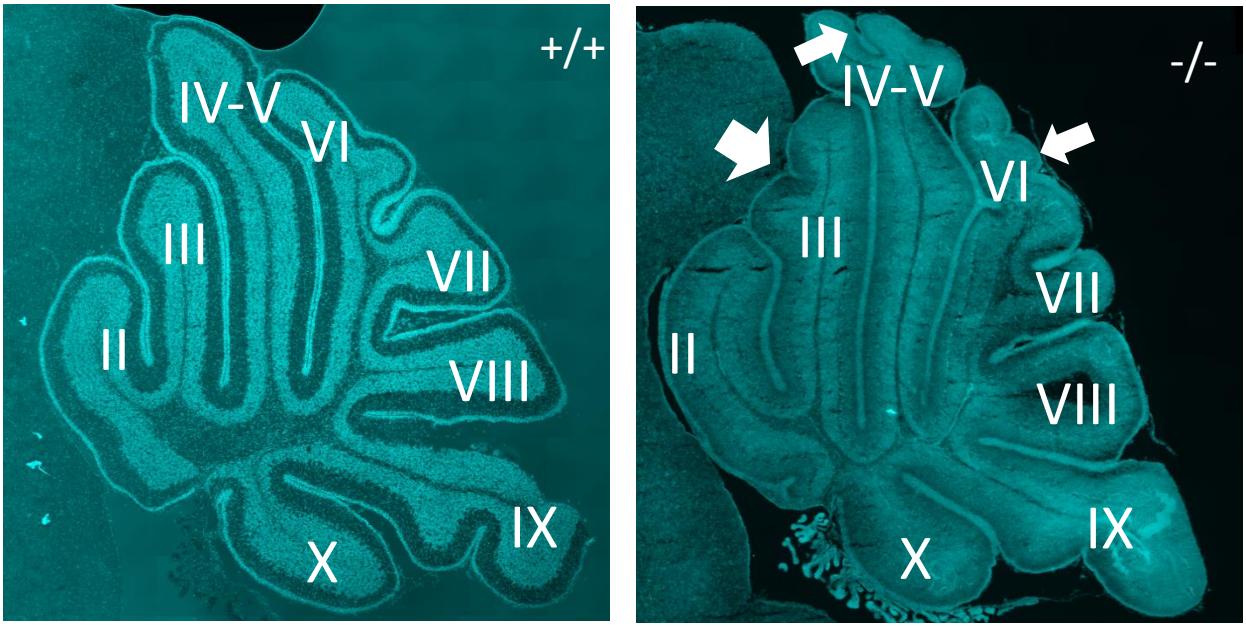

Fig. 11 - We identify ten folia in wild-type and mutant mice. An additional subfolia is identified in mutants at the third, fourth, fifth, and sixth folia. Magnification x5 (Fig. 11 is presented with the consent of Dr. Dimo Stoyanov, MD).

We measured the total area of the slice at different age periods in controls and mutants. At P4, no difference in the total area was found in wild-type mice, compared to mutants. When conducting the Student's t-test, no statistically significant difference was established (p=0.1). The measured area in wild-type individuals was 2.8 sq.mm., and in mutants – 2.7 sq.mm. At P8, no difference in the total area was established in wild-type mice compared to mutants (p=0.12). The measured area in wild-type individuals was 4.1 sq.mm., and in mutants – 3.9 sq.mm. At P12, we also found no difference in total area in wild-type mice compared to mutants

(p=0.12). The measured area in wild-type individuals was 5.9 sq mm, and in mutants – 5.7 sq mm. We also examined the area of the layers in the cerebellar cortex at P12. We found no statistically significant difference in the area of the external granular layer between wild-type individuals and mutants (p=0.189). In wild-type individuals, this area was 0.485 sq mm, and in mutants – 0.507 sq mm.

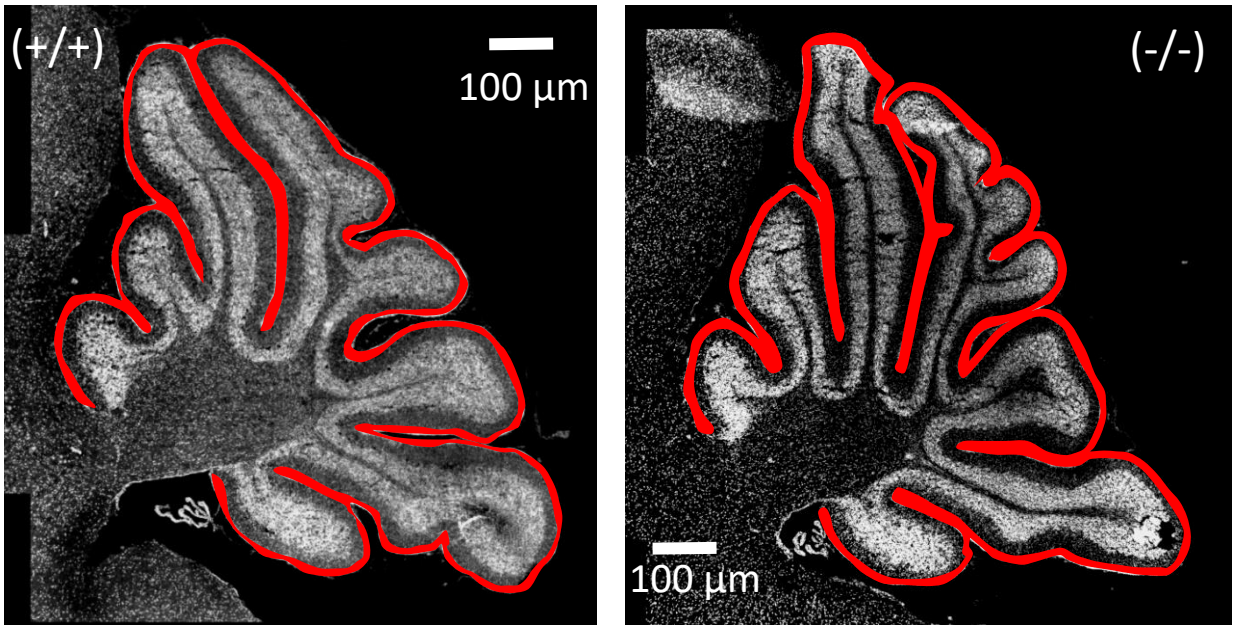

Fig. 12 – Outer granular layer at P12 (wild type on the left side and mutant on the right side).

We also examined the area of the molecular layer at P12. In wild type individuals, this area is 1.373 sq.mm., and in mutants it is 1.425 sq.mm. When performing the Student's t-test (p=0.12). When examining the area of the Purkinje cell layer at the age of P12, we do not find a difference between wild type individuals and homozygous mutants (p=0.2). In wild type individuals, this area is 0.588 sq.mm., and in mutants it is 0.611 sq.mm. We examined the area of the inner granular layer at P12. We find a similar area of this layer in wild type and mutant mice (p=0.28). In wild-type individuals, this area is 2.086 sq. mm, and in mutants it is 2.198 sq. mm. We performed an immunofluorescence study with the neuronal marker Neun to determine the quantity and distribution of neurons in the cerebellum. The aim of our study were the neurons of the inner granular layer. We performed the measurements on cerebellar folia in regions of interest 10,000 μm^2. At P4, we did not find a statistically significant difference in the number of Neun-immunopositive cells between wild-type individuals and homozygous mutants. We observed this both in individual cerebellar folia and as an arithmetic mean for the

entire section (p=0.447). In wild-type and mutant individuals, the largest number of cells was found in the eighth cerebellar folium. The smallest number of cells in wild-type and mutant individuals was found in the third cerebellar folium.

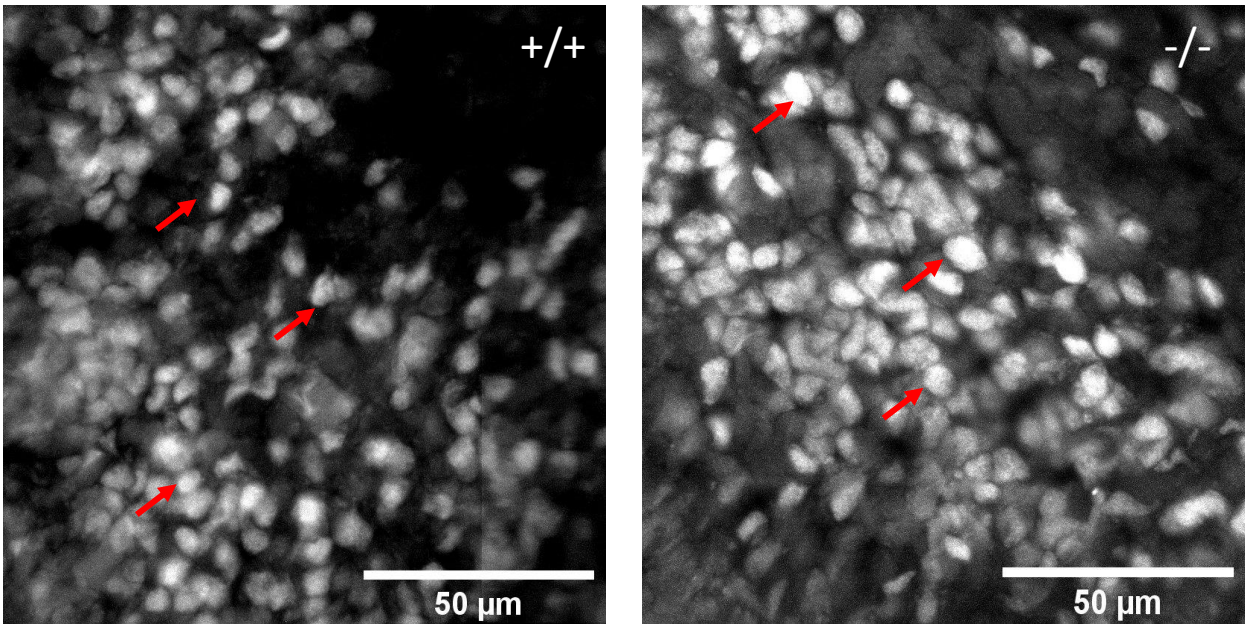

Fig. 13 – Fluorescent images of cerebellar sections of control animals (+/+) and homozygous mutants (-/-) at age P4, illustrating NeuN-immunopositive cells.

At morphological age P8, we did not find a statistically significant difference in the number of neurons in the internal granular layer in wild-type and mutant mice. Arithmetic mean for all folia is p=0.69. In wild-type individuals, we found the largest number of cells in the sixth folium, and in mutants – in the seventh. At P12, we found a similar number of Neun immunoreactive cells in the internal granular layer in wild-type and homozygous mutant mice. Arithmetic mean for all cerebellar folia is p=0.633. The largest number of cells in wild-type and mutant mice was found in the sixth folium.

We also conducted a study with the Calbindin marker to determine the quantity and distribution of Purkinje cells by folia. At age P4, we examined the number of Purkinje cells per folia in areas of interest with an area of 10,000 μm^2. We found a higher number of cells in mutants compared to wild-type mice. We found a statistically significant difference in the third, eighth, ninth and tenth folia ($p<0.05$). In the remaining cerebellar folia $p>0.05$ (Fig. 14).

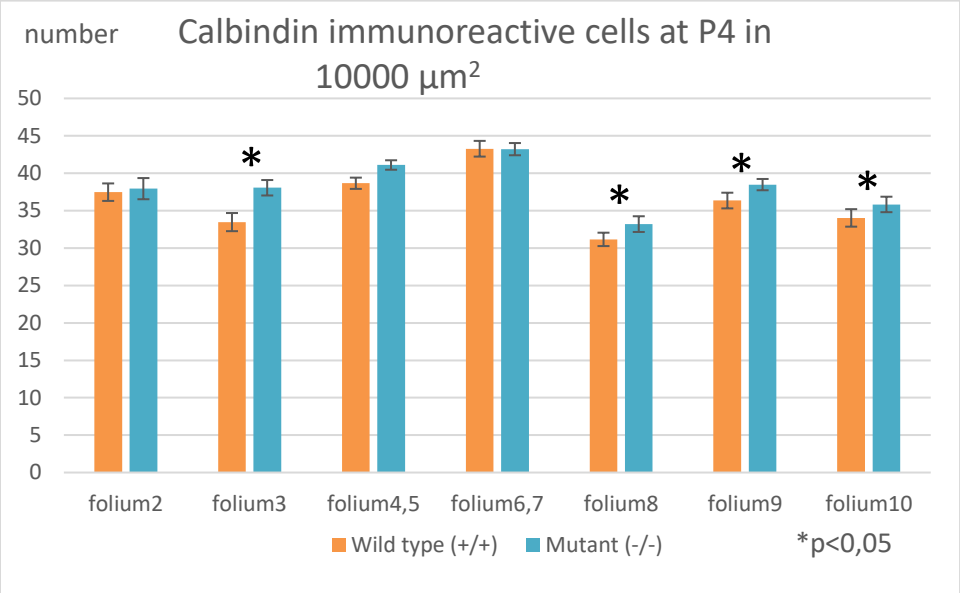

Fig. 14 – Quantitative analysis of the number of CB-immunoreactive Purkinje cells in wild-type and P4 mutant mice. In folia 3, 4-5 and 6-7, a slight predominance of this number was observed in the mutants, while in folia 3, 8, 9 and 10 the difference was statistically significant in favor of the mutants.

We examined the Calbindin – immunoreactive cells of P4 and in 1 mm. length by selecting areas of study randomly, without specifying cerebellar folia. We found a higher number of cells in mutant animals compared to wild-type mice. The difference is statistically significant ($p=0.004$). On the eighth postnatal day (P8) we examined the number of Purkinje cells per folia in areas with an area of 10000 μm^2. We found a slight predominance of the number of cells in mutant animals. We found a statistically significant difference in the third and tenth folia. In these folias $p<0.05$. In the remaining cerebellar folias we did not find a statistically significant difference. Also on P8 we examined the number of Purkinje cells in randomly selected areas with a length of 1 mm. along the entire slice. We found no difference in the number of cells in mutant animals, compared to wild-type mice (controls) ($p = 0.07$). On the twelfth postnatal day (P12) we examined the number of Purkinje cells per folia in areas with a length of 1 mm. We found a slight predominance of the number of cells in mutant animals, compared to wild-type mice (controls). We found a statistically significant difference only in the tenth folium – $p = 0.02$ (Fig. 15).

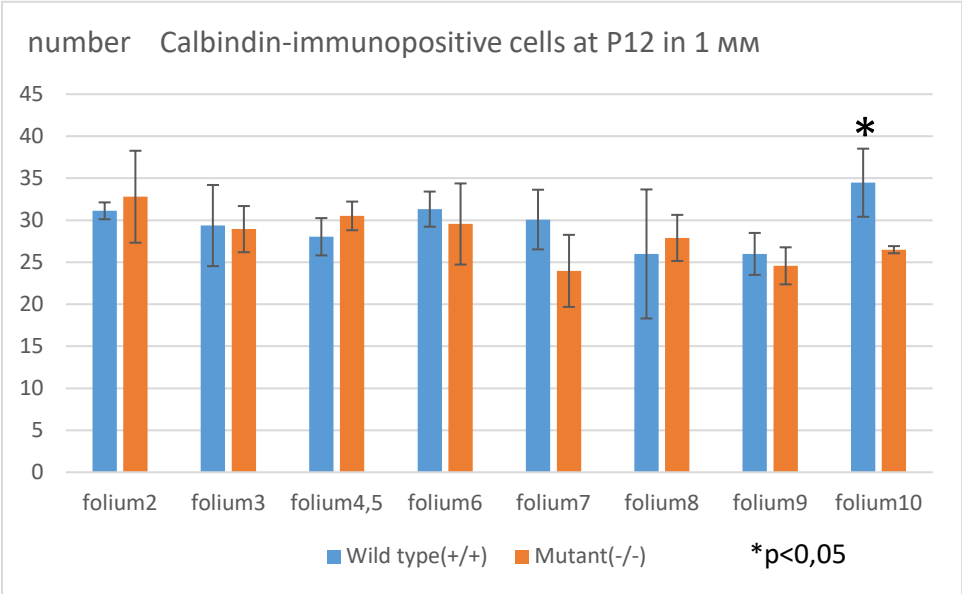

Fig. 15 - Graph comparing the number of Purkinje cells in the two types of experimental animals at P12, along 1 mm. The number of CB-immunoreactive cells in wild-type mice was slightly higher than in mutants at folia 1-9. The only statistically significant difference was seen at folium 10, where controls had 35 cells/mm and mutants had 26 cells/mm (p=0.02).

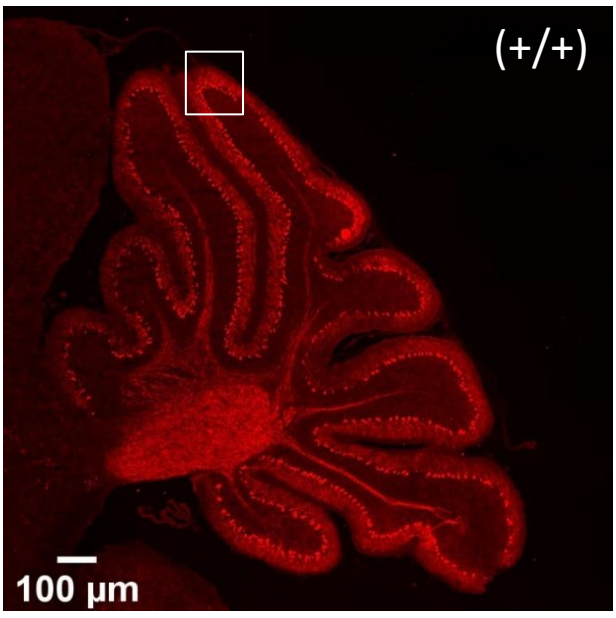

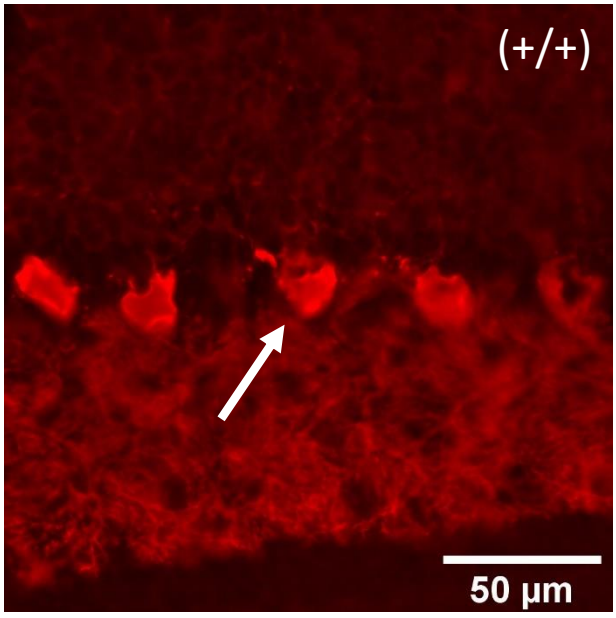

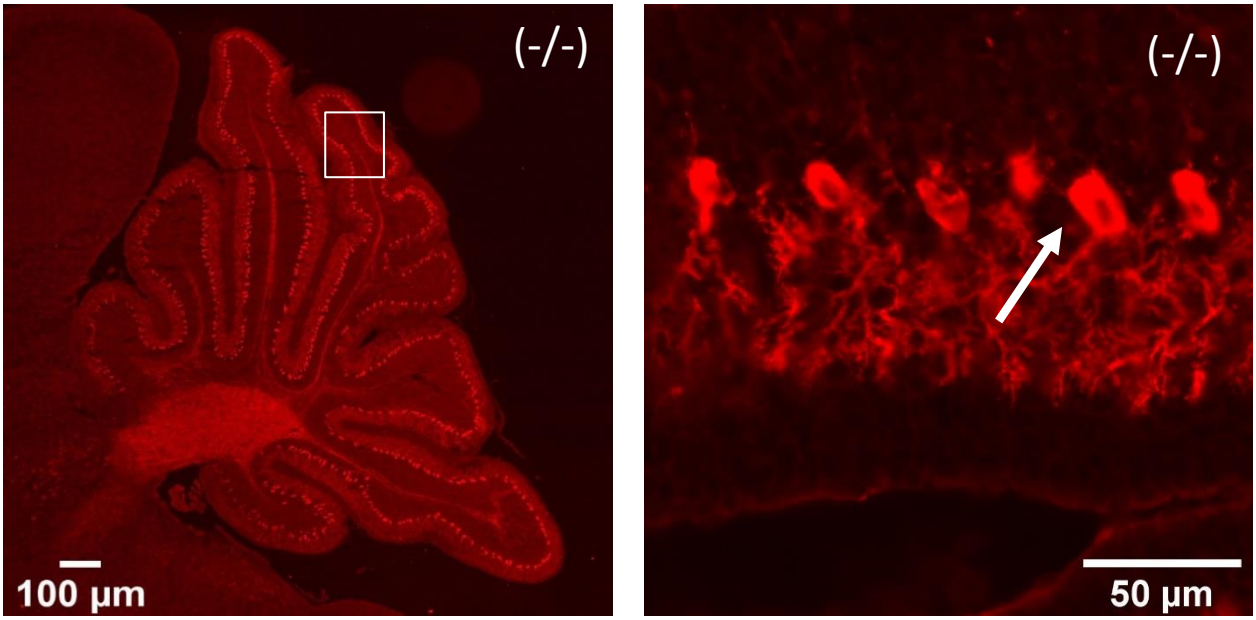

Fig. 16 – Purkinje cells labeled with CB at P12. The upper images are of cerebellar sections from wild-type (+/+) mice, and the lower images are from mutants (-/-). The boxed areas of the low magnification (x5) images on the left are shown in close-up at x40 magnification (right). Individual Purkinje cells are indicated by arrows.

To determine the quantity and distribution of unipolar brush cells across the folia, we performed an immunohistochemical study with the marker Calretinin. At age P4, we found a similar number of unipolar brush cells per whole section in wild-type and mutant mice. When conducting a T-test p = 0.45. We found that Calretinin is preferentially expressed in the last cerebellar folia (ninth and mainly in tenth). We also statistically analyzed the number of cells in the last cerebellar folium at age P4 in study areas with an area of 10,000 μm^2. We found a similar number of unipolar brush cells in wild-type and Zbtb20 knockout mutant mice. The difference is not statistically significant (p= 0.101). In wild-type individuals, we found 50 cells, and in mutants 52 cells. At age P8, we found a similar number of unipolar brush cells per whole section in wild-type and mutant mice, with a slight predominance in mutants. When conducting a T-test, p= 0.24. We found that Calretinin is preferentially expressed in the last cerebellar folia (ninth and mainly in tenth). We also statistically analyzed the number of cells in the last cerebellar folium at age P8 in study areas with an area of 10,000 μm^2. We found a similar number of unipolar brush cells in wild-type and Zbtb20 knockout mutants. The difference is not statistically significant (p= 0.08). In wild-type individuals, we found 70 cells, and in mutants 71 cells.

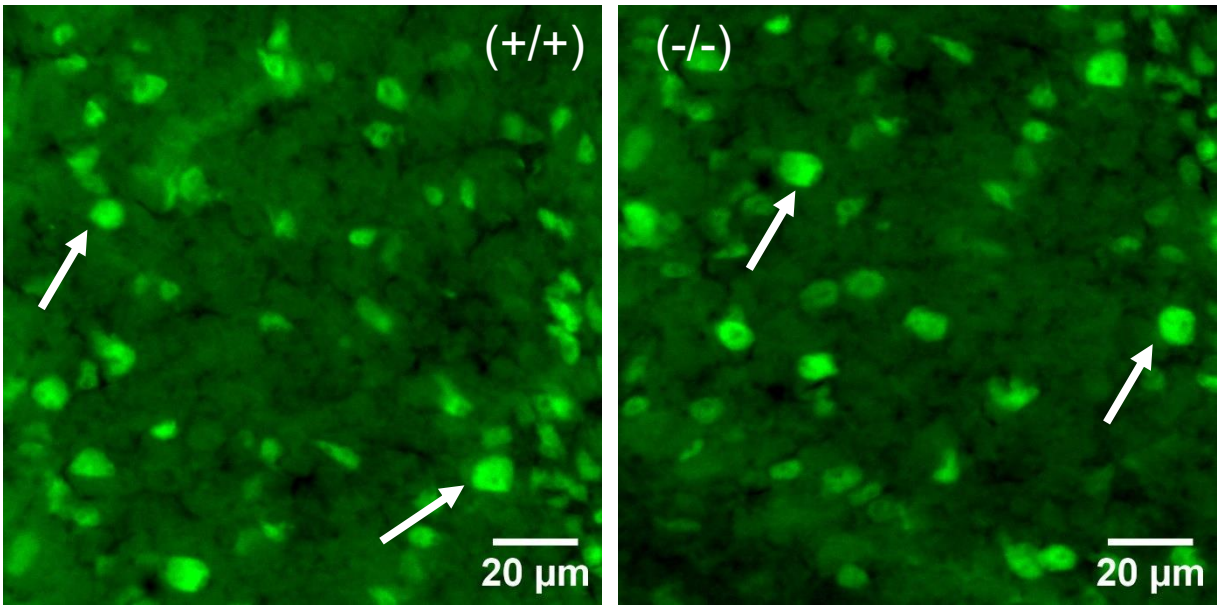

Fig. 17 - Calretinin - immunoreactive cells in wild-type mice (left) and mutants (right), from the area of the tenth cerebellar folium at morphological age P8. Magnification x20.

At age P12, we found a similar number of unipolar brush cells per whole section in wild-type and mutant mice. When conducting a T-test p = 0.23 (Fig. 48). We found that Calretinin is preferentially expressed in the last cerebellar folium (ninth and mainly in the tenth). We also statistically analyzed the number of cells in the last cerebellar folium at age P12 in regions of interest 10,000 μm^2. We found a similar number of unipolar brush cells in wild-type and Zbtb20 knockout mice. The difference is not statistically significant (p = 0.06). In wild-type individuals, we detect 68 cells, and in homozygous mutants, 73 cells.

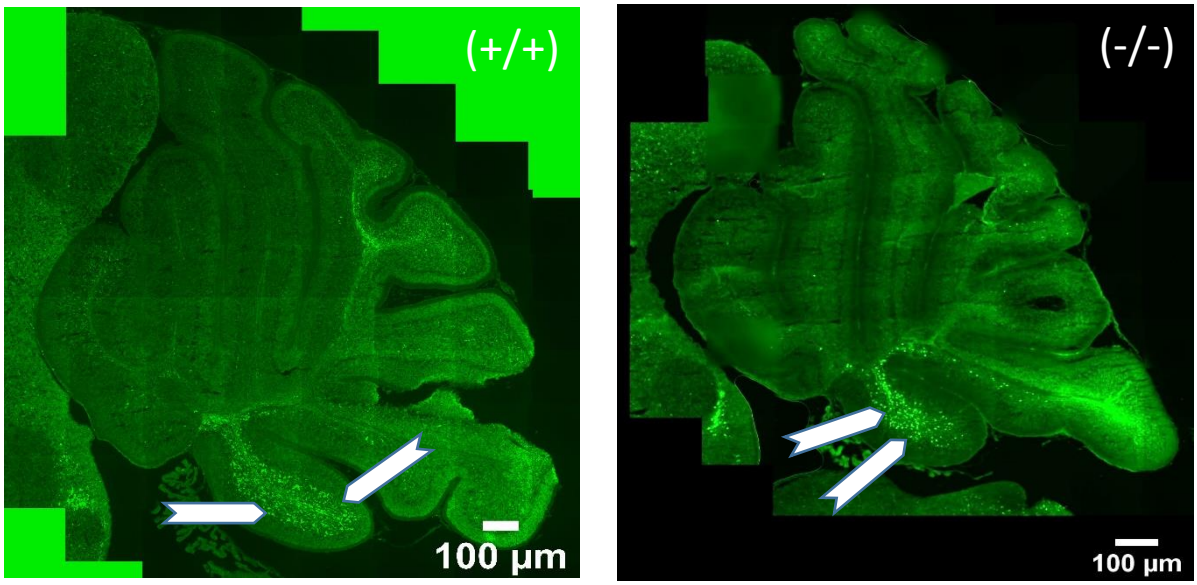

Fig. 18 - Overview photographs of identical cerebellar sections from wild-type (+/+) and mutant (-/-) mice at P12, illustrating the location of CR+ unipolar brush cells (arrows) predominantly in the tenth cerebellar folia. Magnification x5.

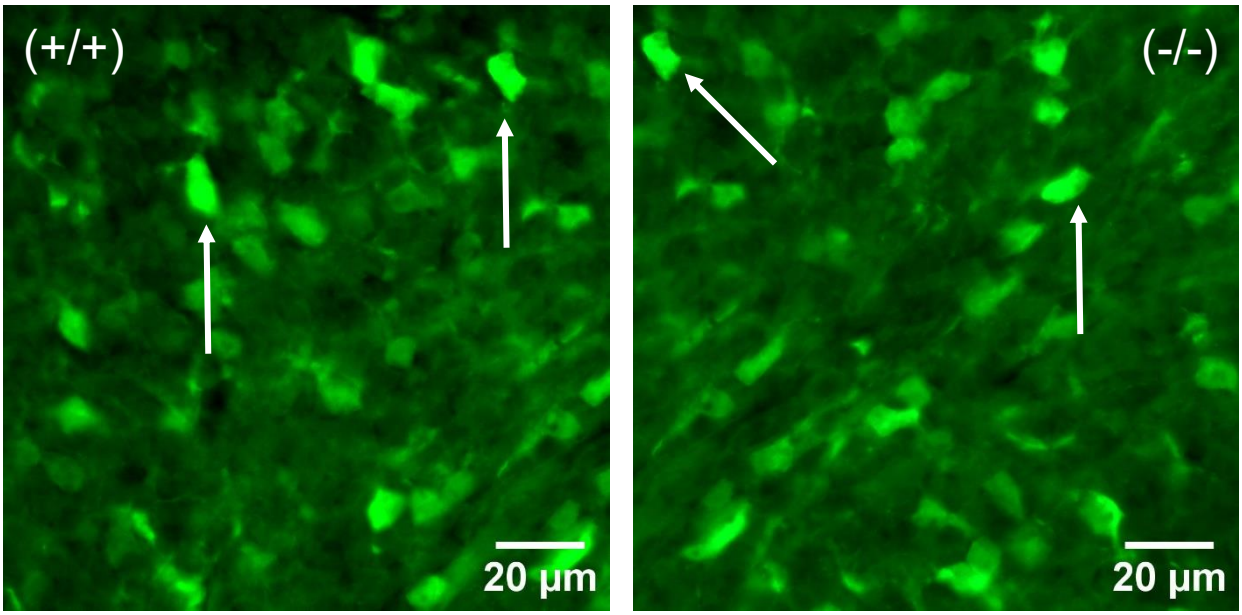

Fig. 19 - Close-up of CR-immunoreactive cells (arrows) in wild-type (+/+) and mutant (-/-) mice in the region of the tenth cerebellar folium at P12. Magnification x20.

To determine the quantity and distribution of Golgi type II cells in the cerebellar cortex, we performed immunofluorescence staining with the Pax2 marker. At P4, we examined the distribution of Golgi type 2 cells in cerebellar folia in study areas with an area of 10,000 μm^2.

We found no difference in the number of cells in wild-type mice compared to mutants (p=0.29). At P8, we examined the number of Golgi type II cells in study areas with an area of 10,000 μm^2. We found no difference in the number of cells in wild-type mice compared to mutants (p=0.5).

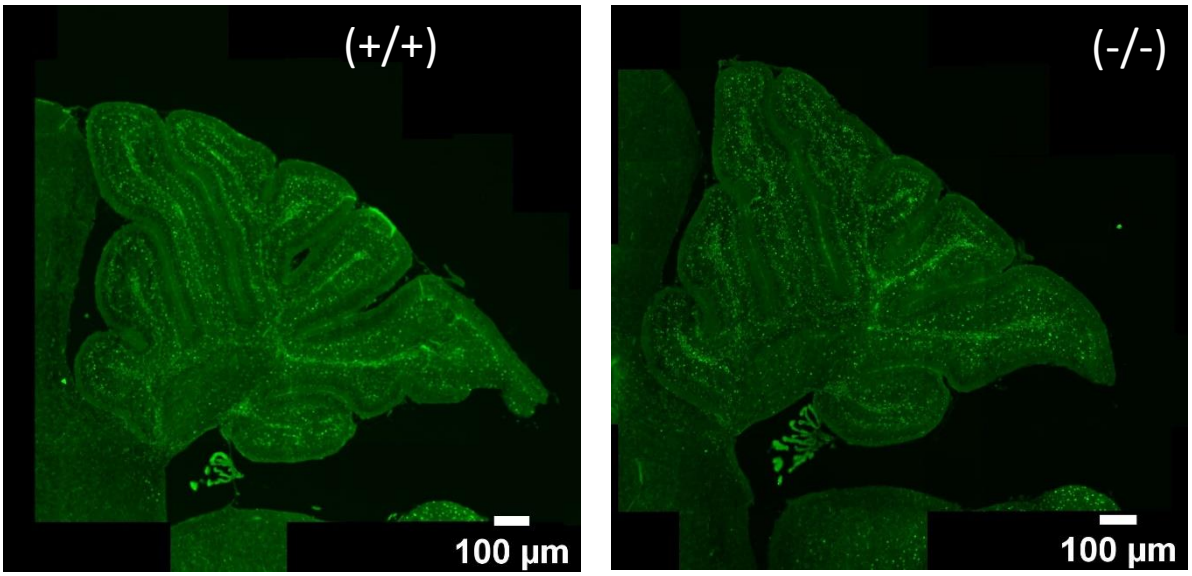

Fig. 20 – Overview fluorescence micrographs of analogous sections from wild-type (+/+) and mutant (-/-) mouse cerebellum illustrating the distribution of Pax2-immunoreactive cells at age P8. Magnification x5.

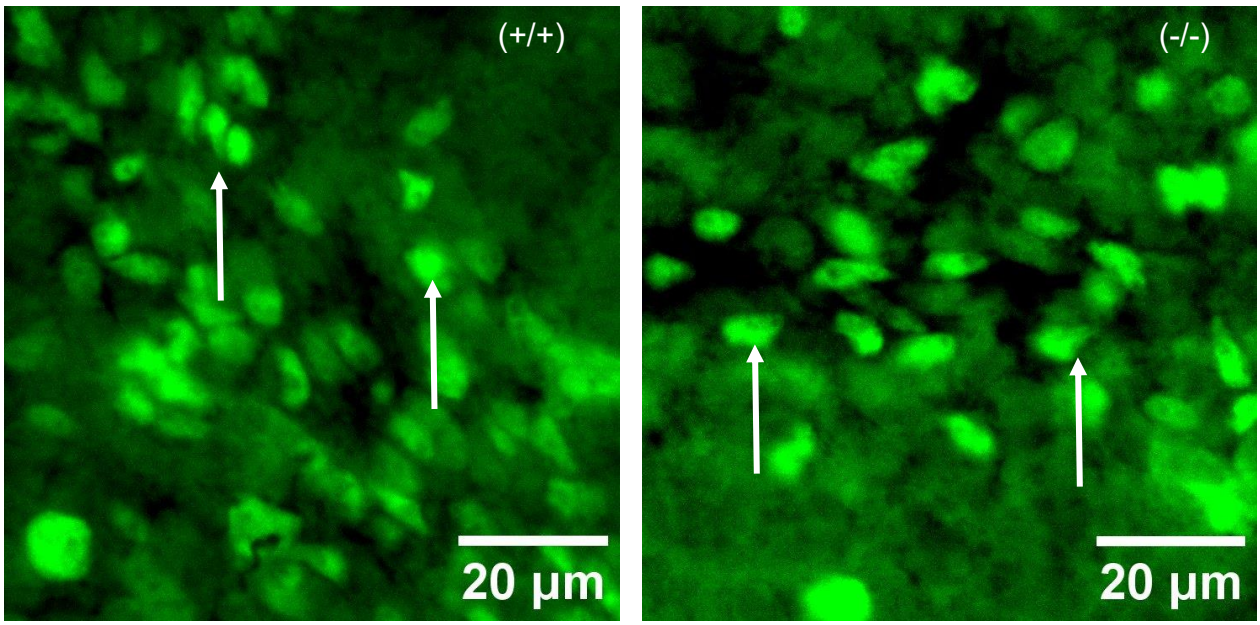

Fig. 21 – Pax2 – immunoreactive cells at age P8 from the area of the fourth cerebellar folium. Wild-type individual (left) and mutant (right). Magnification x 20.

At morphological age P12, we analyzed the number of Golgi type 2 cells in study areas with an area of 10,000 μm2. We did not find a statistically significant difference in the number of cells between wild-type and mutant mice (p=0.4).

To determine the number and distribution of proliferating cells in the cerebellum, we performed immunofluorescence staining with the marker Ki-67. We conducted a study of the number and distribution of Ki-67 immunoreactive cells in similar areas with an area of 10,000 μm2 in wild-type and mutant mice. We conducted the study along the entire cerebellar folium, within the molecular and external granular layers, at the three age periods. At age P4, we found a similar number of proliferating cells in wild-type and mutant individuals (p=0.53). At age P8, we found a similar number of proliferating cells in wild-type and mutant individuals (p=0.34).

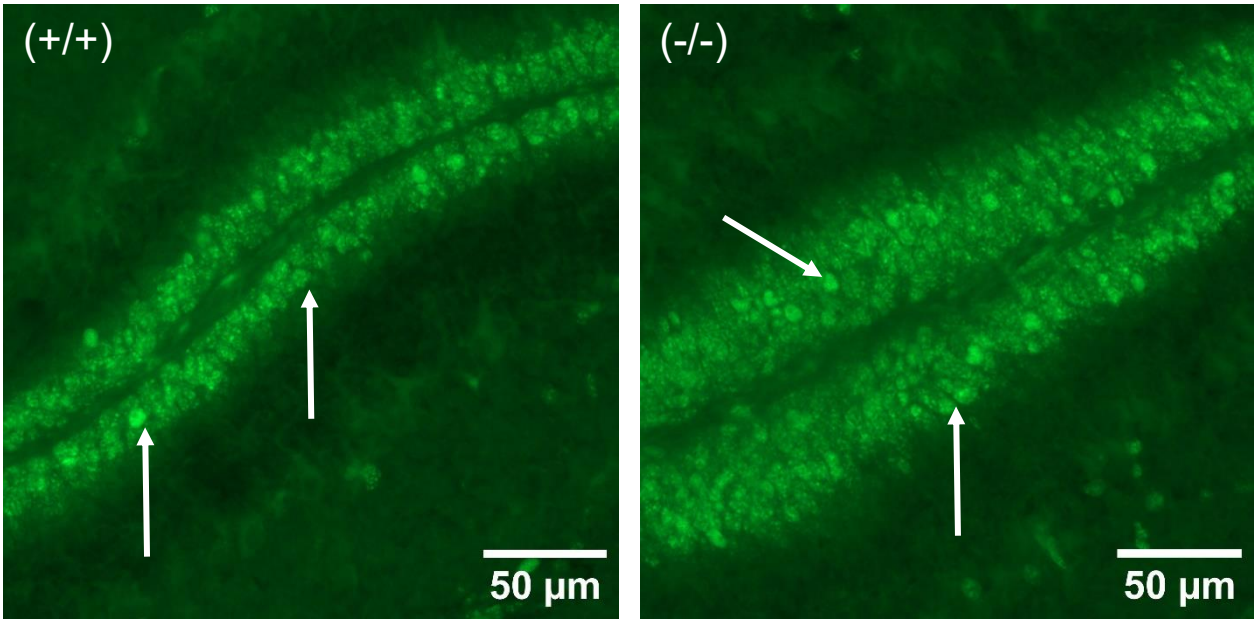

Fig. 22 - Close-up dark-field micrographs of cortical sections illustrating the presence of Ki-67-immunopositive cells (arrows) in a wild-type (+/+) and mutant (-/-) P8 mouse. Magnification x20.

At age P12, we found a similar number of proliferating cells in wild-type and mutant individuals (p=0.52). On both age periods there was a weak prevalence in the wild type mice.

To determine the quantity and distribution of proliferating cells in the cerebellum, we performed immunofluorescence staining with Ki-67 at morphological age P12. We focused on the quantity and distribution of Ki-67 immunoreactive cells in similar areas with an area of

10,000 μm^2 in wild-type and mutant mice. The areas are along the entire cerebellar folium, within the molecular and external granular layers at age P12. In the same areas, we also examined DAPI – immunopositive cells. We calculated the percentage ratio between Ki-67 immunoreactive cells and DAPI immunopositive cells. We found a statistically significant difference in the second, fourth, fifth, sixth, ninth and tenth cerebellar folia. In these folias there is a predominance of proliferating cells in mutants and when conducting the Student's test $p<0.05$. In the remaining folias we did not find a statistically significant difference.

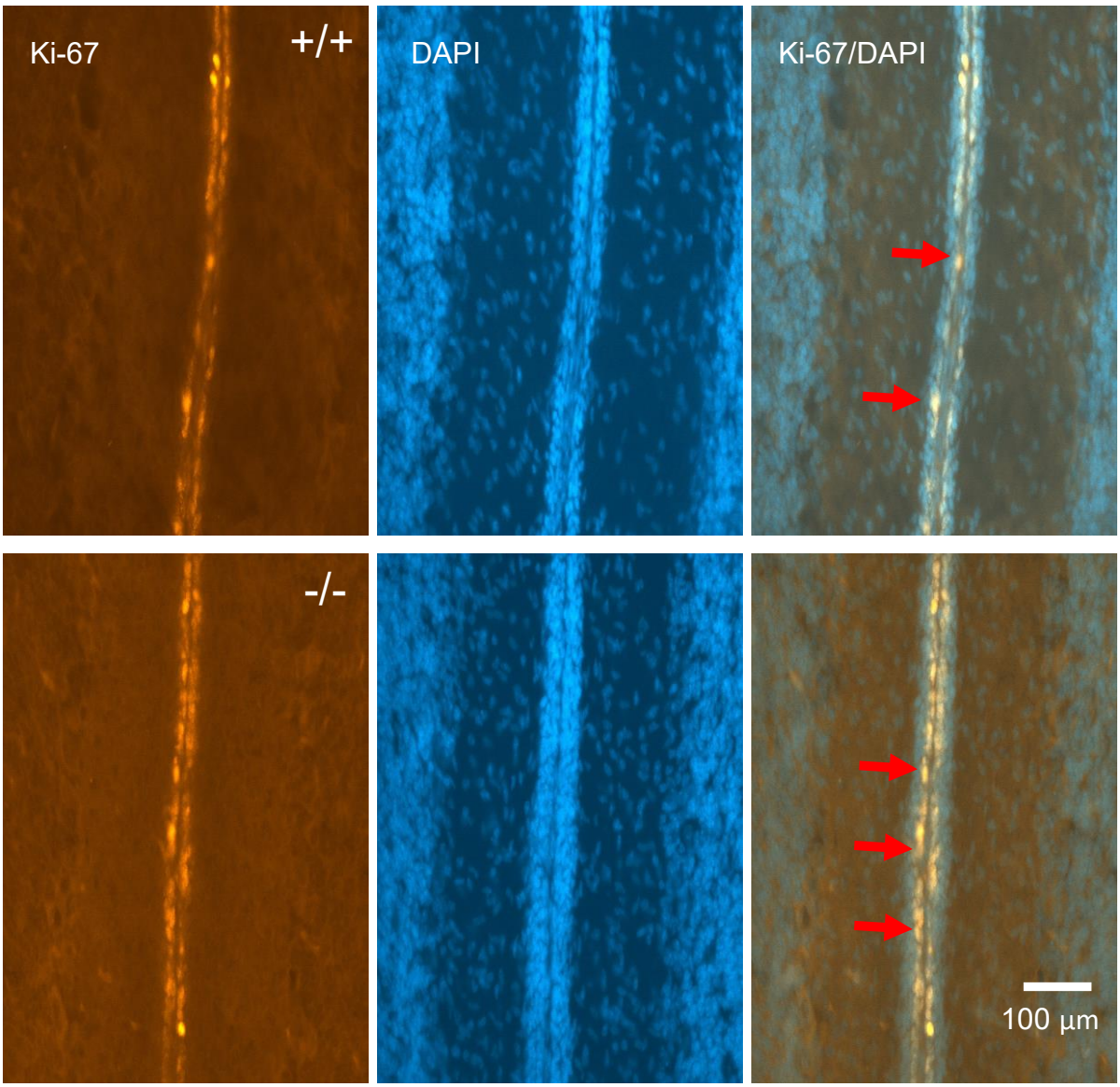

Fig. 23 – Proliferating cells (arrows) from the region of the fourth and fifth cerebellar folia in a wild-type (+/+) and mutant (-/-) mouse, in greater numbers in the mutants. Magnification x40.

In order to determine the quantity and distribution of granular neurons in the external granular layer, we performed a study with the Pax6 marker. We conducted the analysis in all cerebellar folia in similar areas with an area of 10,000 μm^2 in wild-type and mutant mice at the age of P12. We found a statistically significant difference in the sixth and tenth cerebellar folia ($p<0.05$). In these, a greater number of granular neurons are found in wild-type individuals compared to mutants. We studied the average number of Pax-6 immunopositive cells in all cerebellar folia in study areas of 10,000 μm^2. We did not find a statistically significant difference between wild-type and mutant individuals ($p=0.24$). We also examined the thickness of the outer granular layer in folia in wild-type and mutant individuals, also using the Pax6 marker. We found a statistically significant difference in the fourth, fifth, eighth, ninth and tenth cerebellar folia. In these folia, $p<0.05$. In the remaining cerebellar folia, we did not find a statistically significant difference (Fig. 24).

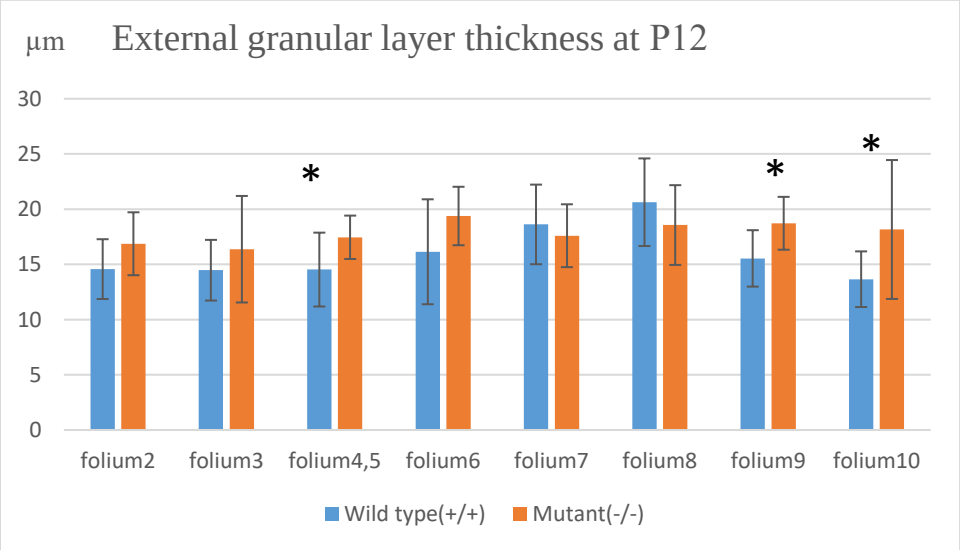

Fig. 24 – Graph reflecting the thickness of the outer granular layer on foils of P12. * indicates data whose differences are statistically significant

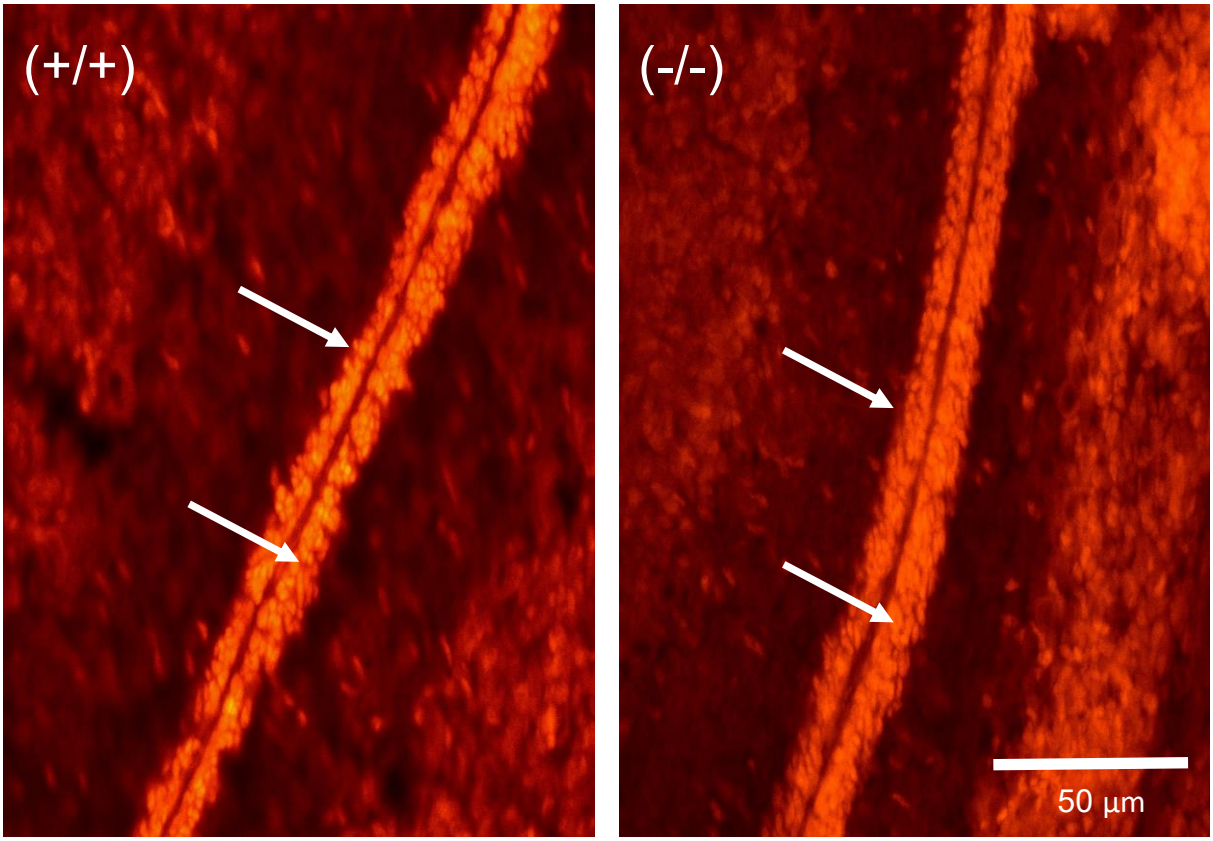

Fig. 25 – Outer granular layer in the region of the fourth and fifth folia in a wild-type mouse on the left and a mutant on the right. We have found a greater thickness of this layer in mutant animals. Magnification x 40.

We investigated the average thickness of the outer granular layer, analyzing all cerebellar folia together and calculated the arithmetic mean value for the entire slice. We did not establish a statistically significant difference in the thickness of the outer granular layer at the age of P12 between wild-type individuals and homozygous mutants (p=0.1).

To perform a quantitative analysis of astrocytes in the cerebellum, we performed an immunofluorescence study with the GFAP marker. We measured the GFAP-immunopositive area of the entire slice. We compared this area with the total area of the cerebellar slice. At the age of P4, we did not establish a difference in the area between wild-type individuals and mutants (p=0.11). When comparing the ratio of GFAP-immunopositive area to the area of the entire slice between controls and mutants, we found that there was no statistically significant difference between wild-type and mutant individuals (p=0.4). In wild-type individuals, 8.53% of the total area of the slice was GFAP-immunopositive, and in mutants, 8.32% of the total area of the slice was GFAP-immunopositive. At age P8, we found a similar GFAP-immunopositive area of the entire slice in wild-type and mutant mice (p=0.1). In wild-type individuals, it was

0.38 sq.mm., and in mutants, it was 0.396 sq.mm. When comparing the ratio of GFAP-immunopositive area to the area of the entire slice between controls and mutants at P8, we found that this ratio was similar (p=0.07). In wild-type individuals, 13.3% of the total area of the slice was GFAP-immunopositive, and in mutants, 14.45% of the total area of the slice was GFAP-immunopositive. At age P12, we did not find a difference in the GFAP-immunopositive area of the entire slice between wild-type and mutant mice (p=0.4). In wild-type individuals, it was 0.788 sq.mm., and in mutants, it was 0.884 sq.mm. We did not find a difference in the ratio of GFAP-immunopositive area to the entire slice area between controls and mutants at age P12 (p=0.1). In wild-type individuals, 14.32% of the total area of the slice was GFAP-immunopositive, and in mutants, 16.74% of the total area of the slice was GFAP-immunopositive.

To determine the quantity and distribution of oligodendrocytes in the cerebellum, we performed a study with the marker Olig2. We conducted the study in all cerebellar folia in similar areas with an area of 10000 μm^2 in wild-type and mutant mice at the age of P12. We found a statistically significant difference in the third, sixth and seventh cerebellar folia ($p<0.05$). In them, a greater number of Olig2-immunopositive cells were found in mutants compared to wild-type individuals. In the remaining cerebellar folia, no statistically significant difference was found. We also analyzed the average number of oligodendrocytes for all folia at the age of P12. We did not find a statistically significant difference between wild-type individuals and homozygous mutants (p=0.22). In wild-type individuals, we found 12 cells, and in mutants, 14 cells.

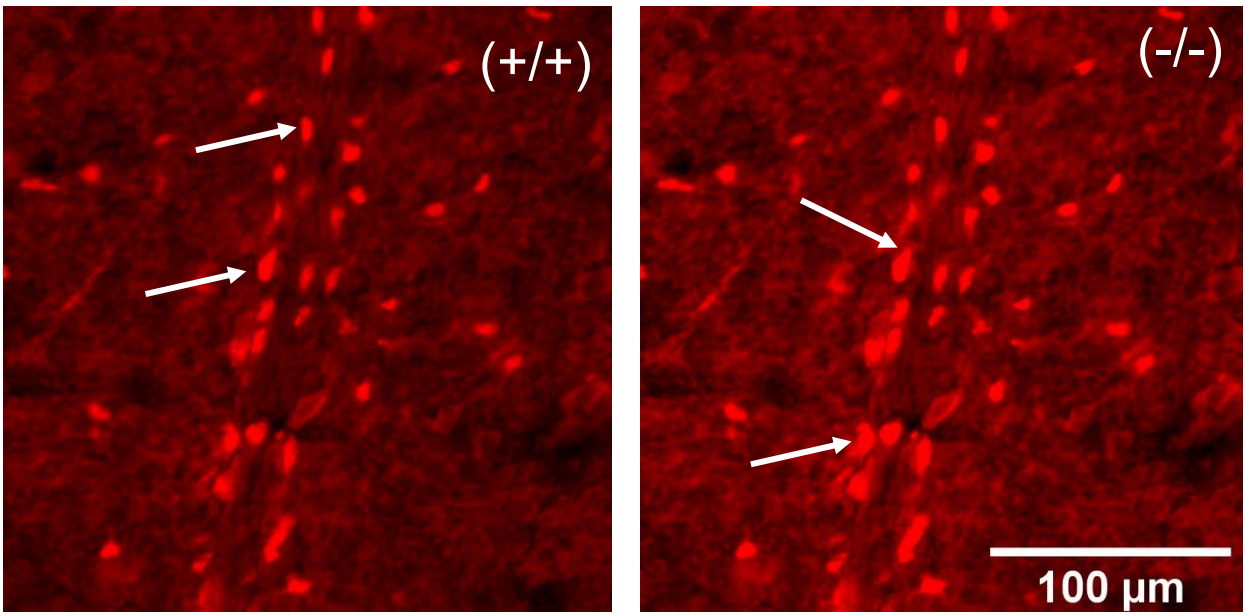

Fig. 26 – Images from the third cerebellar folia region of a control (+/+) and a homozygous mutant (-/-) at P12, demonstrating expression of the neuroglial marker Olig2. Positive cells (arrows) are stained red. Magnification x40.

To determine whether there is expression of Zbtb20, we performed an immunofluorescence study with this marker at the three age periods (P4, P8 and P12) in wild-type and mutant mice. In wild-type mice, we found expression of this marker, while in homozygous Zbtb20-/- mice, we did not find expression of the marker. At age P4, we performed a study on cerebellar folia in regions of interest in 10,000 μm^2. The largest number of cells in wild-type mice is found in the sixth and seventh folium – 39 cells. In mutants, we did not find the presence of Zbtb20 – immunoreactive cells. A statistically significant difference between wild-type and mutant individuals was found in all cerebellar folia ($p<0.05$).

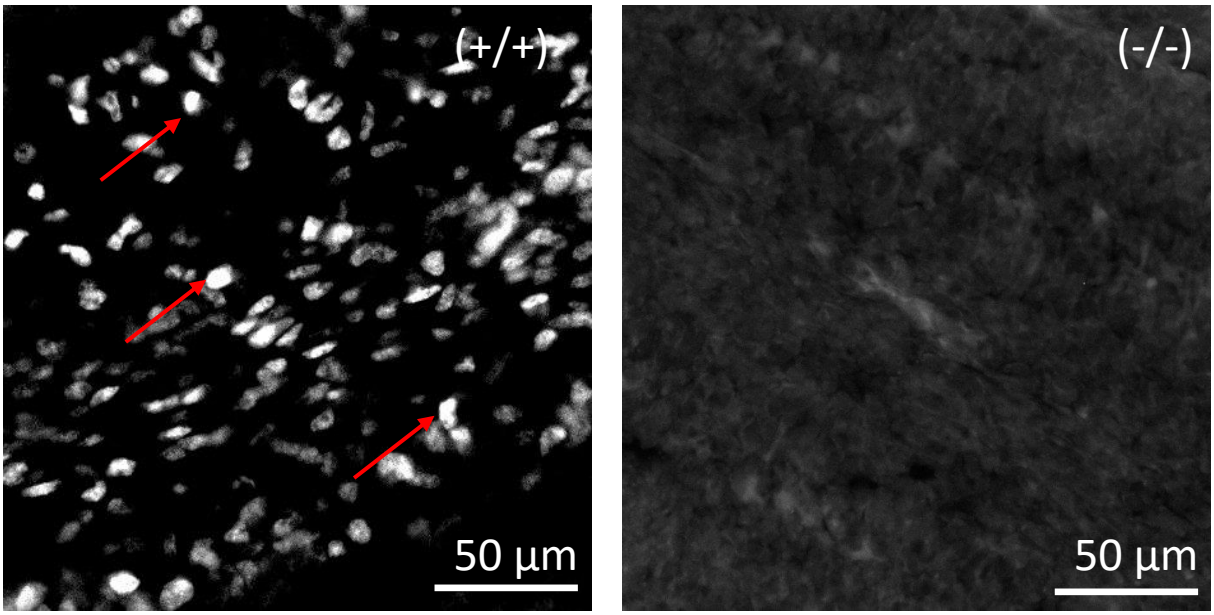

Fig. 27 – Expression of Zbtb20-immunoreactivity at age P4. Positive cells are observed only in wild-type (+/+) mice, while cerebellar sections of knockout mutants (-/-) are negative. Magnification x40.

At age P8, we conducted a study on cerebellar folia in study areas with an area of 10,000 μm^2. The largest number of cells in wild-type mice is detected in the third folium – 27 cells. In mutants, we do not detect the presence of Zbtb20 – immunoreactive cells. A statistically significant difference between wild-type and mutant individuals is detected in all cerebellar folia ($p<0.05$).

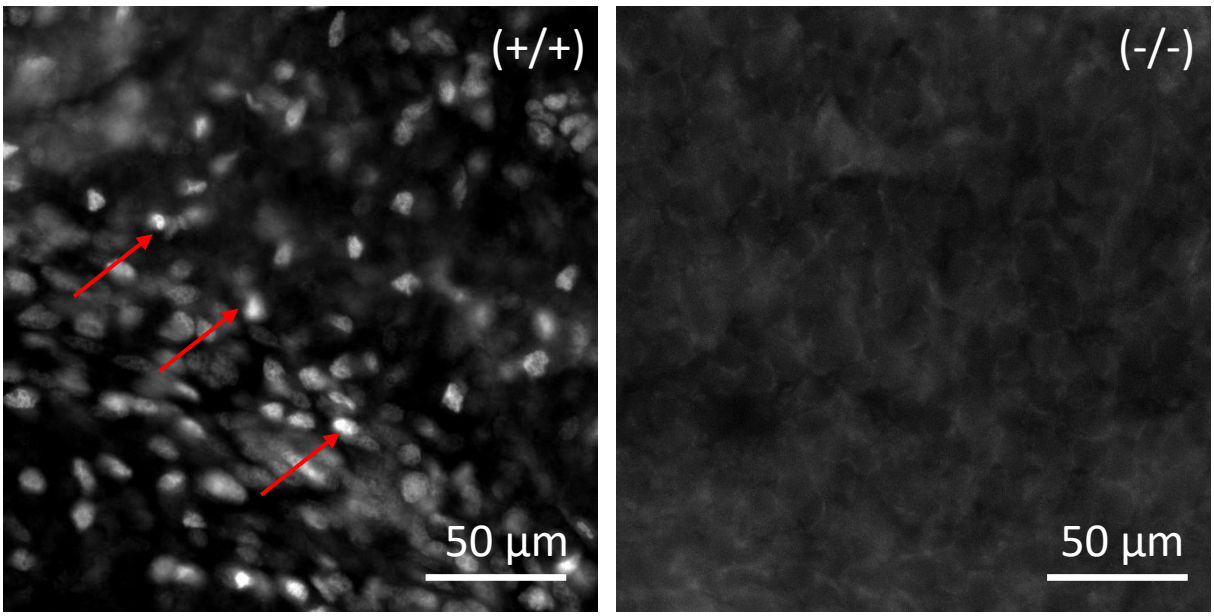

Fig. 28 – Zbtb20-immunoreactive cells in control animals at P8 age are observed only in wild-type (+/+) mice. Knockout mutants (-/-) do not express the transcription factor. Magnification x40.

At age P12, we conducted a study on cerebellar folia in study areas with an area of 10,000 μm^2. The largest number of cells in wild-type mice is detected in the second folium – 36 cells. In mutants, we do not detect the presence of Zbtb20 – immunoreactive cells. A statistically significant difference between wild-type and mutant individuals is detected in all cerebellar folia ($p<0.05$).

Implications:

1. In the postnatal period, and more precisely at P4, P8, P12 and P30, Zbtb20 is expressed by neuroglial cells (oligodendrocytes, Bergmann glia and astrocytes). Neurons do not express Zbtb20.
2. The transcription factor Zbtb20 affects the development of the cerebellar folia. In the absence of Zbtb20, additional folds are observed in some of the cerebellar folia at the age of P4, P8 and P12.
3. Zbtb20 does not regulate the size and area of the cerebellum in the postnatal period.
4. Zbtb20 selectively affects the amount of proliferating cells in the cerebellum. The absence of the transcription factor leads to a significant increase in the percentage of Ki67-positive cells in folia 4-5, 6 and 10 at P12.
5. The lack of Zbtb20 affects the proliferation of Purkinje cells selectively in terms of time and location: at P4, mutants show an increased total number of cells expressing CB per 10,000 μm^2, as well as a selective increase in folia 3, 8, 9 and 10; at P8, the number of Purkinje cells is increased only in folia 3 and 10; at P12, this effect is absent and even in folia 10, the number of Purkinje cells is significantly lower than in controls.
6. The lack of Zbtb20 does not change the total number of granule cells (Pax6+), but leads to their significant reduction in folia 6 and 10 at P12.
7. Zbtb20 probably suppresses the development of the outer granular layer selectively in certain areas of the cortex: at P12 in mutants, the layer thickness is greater in folia 4-5, 9 and 10.
8. The transcription factor Zbtb20 probably affects the migration of granular glutamatergic neurons from the outer granular layer to the inner granular layer at P12. The absence of this factor is associated with a delayed migration of these neurons to the inner granular layer.
9. Zbtb20 does not regulate the thickness of the molecular and inner granular layers.
10. Zbtb20 does not affect the proliferation of unipolar brush-type neurons (CR+) in the postnatal cerebellum.
11. Zbtb20 does not affect the proliferation of Golgi cells (Pax2+) after birth.
12. Zbtb20 is not involved in regulating the proliferation of excitatory interneurons (Tbr2+) in the cerebellum.
13. Zbtb20 has no effect on the proliferation of astrocytes in the cerebellum in the postnatal period.

14. Zbtb20 selectively suppresses the proliferation of oligodendrocytes in the postnatal period of cerebellar development: in P12 mutants, the number of oligodendrocytes is significantly increased in folias 3, 6 and 7.

Discussion

In our studies, we identified Zbtb20 expression in the cerebellum of wild-type mice. At postnatal day 30, this marker is expressed by neuroglial cells (oligodendrocytes, Bergmann glia, and astrocytes). The neuronal cell population does not express Zbtb20. To the best of our knowledge from the available literature, no such study on the role of Zbtb20 and its expression in the cerebellum has been conducted to date.

It has been established that isoforms of the BTB/POZ domain of Pach have a role in the development of hippocampal neurons, cerebellar granular neurons, neuroglial progenitors, and differentiated neuroglia. These isoforms are called HOF^{L} and HOF^{S}. HOF is transiently expressed during postnatal life in the granular layer of the cerebellum. By P15, HOF is expressed in a small cell population of the molecular layer, cells that line the pia mater. By P20, HOF expression in the internal granular and molecular layers decreases sharply. These data indicate that HOF is transiently upregulated in the nuclei of migrating precursors of granule neurons. As granule neurons mature in the internal granular layer, gene expression decreases sharply (Mitchelmore, Cathy et al., 2002). Zbtb20 is expressed at E9.5 in the somites, and from E10.5 onwards in the neural tube and developing skeleton (Ikeya and Takada 2001). This transcription factor determines the differentiation of GABAergic and glial stem cells in the cerebellum. GABAergic neurons in the cerebellum are a relatively large cell population. They include Purkinje cells, inhibitory interneurons of the cerebellar nuclei, stellate and basket cells, and Golgi cells. Zbtb20 mutations are found in diseases related to the development of the central nervous system. They are thought to affect the function of neurons that are important for learning, memory and behavior. Such diseases include autism and Primrose syndrome (Casertano A, Fontana P, et al. 2017). Overexpression of the transcription factor causes defects in the formation of cortical layers, and reduced function leads to reduced dendritic arborization (Xie Z, Ma X, et al. 2010).

Zbtb20 mutations differentially affect synaptic structure (Kelly A Jones, Yue Luo, et al. 2018). The P46R variant, which has been shown to be associated with autism risk, changes the size of dendrites, suggesting a role for the N-terminus of Zbtb20 in regulating synaptic structure. The G346V variant induces expansion of the basal part of dendrites, and the A620V variant leads to expansion in the terminal region. A mutation without the C-terminal domain alters the apical and basal parts of dendrites. It has been suggested that modulation of apical or basal dendritic arborization can alter the synaptic contacts of a given neuron and lead to impaired neurological development (Jan YN, Jan LY, 2010).

Variants of the same protein can contribute to different disease states by disrupting neuronal structure or synaptic contacts in a specific way. A family of BTB domain-containing proteins controls axonal outgrowth (Kim TA, Jiang S, et al. 2005). Subtle changes in dendritic or synaptic structure can lead to major changes in information processing (Chen JL, Nedivi E. 2010). Dendritic morphology and arborization are determinants of neuronal function and are impaired in many neurological diseases affecting behavioral and intellectual functions (Li W, Wang F, et al. 2004). Zbtb20 influences the dendritic and synaptic structure of pyramidal neurons in the forebrain. Genetic disorders may play a role in the expression of diseases related to the development of the CNS (Kelly A Jones, Yue Luo, et al. 2018).

Zbtb20-specific regions are absent in brain samples from Zbtb20-/- experimental animals. This confirms the lack of Zbtb20 expression in the knockout model. The hippocampal neuron-specific antibody HPA015551 detects anti-Zbtb20 labeling exclusively in wild-type neurons, and is absent in mutants (Ripamonti S, Shomroni O, et al. 2020). In our study on Zbtb20-/- mice at P4 and P8, we did not find Zbtb20 immunopositive cells, while positive cells were observed in controls. At P12, we found Zbtb20+ cells in controls, and no cells in mutants. These data give us reason to believe that Zbtb20 is not expressed in the early stages of postembryonic development in Zbtb20-/- mice.

When examining the foliation of the cerebellum, we found a similar number of cerebellar folia in wild-type individuals and in mutants at the corresponding postnatal age. At P4, P8 and P12, we found ten cerebellar folia in both wild-type individuals and mutant mice. At P8 and P12, in mutants in the region of the third, as well as in the fourth and fifth folia we observed an additional cerebellar subfolium. At P12, a similar additional folding also appears in the sixth folia, again in mutants. This additional folding is probably due to the lack of the transcription factor Zbtb20. As far as we know from the literature, such a study on Zbtb20-/- mutants has not been conducted so far.

Foliation was studied in Shh knockout mutants. Granule neuron precursors proliferate until birth and shortly thereafter. At this stage, foliation is not established. Foliation in Shh knockout mutants is with the formation of additional furrows and elongated lobes. Shh does not determine the position of the fissures, nor the differential patterning of the vermis and hemispheres, but Shh is the triggering factor for foliation. The positioning of the fissures is determined by the relationship between Purkinje cells and mossy fibers, as well as by the fibers of granule neurons (Corrales, Blaess et al. 2006).

Selective elimination of GCPs in the late embryonic period or early postnatal stages in rats (Doughty et al., 1998) leads to the formation of fewer foliations. Minimal expression of Shh is

required for the initial phases of lobulation (Corrales, 2006). Shh -/- mutants show a lack of foliation. Low expression of Shh results in incomplete cerebellar foliation, while overexpression of Shh results in hyperfoliation. The size of the cerebellum also increases in association with the enhanced foliation (Corrales, Blaess et al. 2006).

When examining the area of the cerebellum, we found that the total area of sections at P4, P8 and P12 was similar in wild-type and mutant individuals. At the same time, at P8 and P12 we also found additional folds in folia three, four and five. At P12, an additional subfolium also appears in folia six. It is likely that the transcriptional repressor Zbtb20 affects the formation of additional folds, but does not affect the size of the cerebellum. As far as we know from literature data, a similar study of the size and area of the cerebellum on Zbtb20-/- experimental animals has not been conducted so far.

Examining the area of the molecular layer at P12, we found that it was similar in wild-type and mutant mice. This suggests that the transcription factor Zbtb20 does not affect the development of the molecular layer in the postnatal period. There is no data in the available literature on a similar study on Zbtb20-/- mice.

From our studies, we found that with advancing age, the thickness of the outer granular layer gradually decreases. We observed this pattern in both wild-type and mutant mice. This is associated with the migration of granular neurons from the outer granular layer to the inner granular layer. To our knowledge, such a study has not been conducted on Zbtb20-/- experimental animals.

According to (Bovio PP, et al., 2018), Dot1l-/- mice have a smaller outer granular layer in area, as well as a smaller number of precursors of granular neurons. There is also a disturbance in the proliferation and differentiation of granular progenitors. This leads to a smaller brain size. When conducting motor behavior tests, the animals exhibit ataxia.

By examining the area of the outer granular layer, molecular, inner granular and Purkinje cell layers at P12, we found that it is similar in wild-type and Zbtb20-/- mutant mice. It is likely that the transcription factor Zbtb20 does not affect the development of these layers of the cerebellar cortex. Such a study has not been conducted so far.

Ma D et al. (2020) created a mouse model with Down syndrome and observed a reduced thickness of the cerebellar cortex. This is due to thinning of the inner granular layer. The area of the cortex is also reduced, which is due to the reduced area of the molecular layer. According to (Landis DM, 1978) from P3 to P21, the thickness and area of the outer granular layer in mutant (staggerer) mice gradually decreases. The number of postmitotic granular neurons also decreases.

Our study found that Purkinje cells at P4 are more numerous per unit area in mutants. At P8 and P12, we find similar numbers of cells in mice from both experimental groups. It is likely that in the early postnatal period, the transcription factor Zbtb20 transiently suppresses the proliferation and migration of Purkinje cells. To the best of our knowledge from the literature, such a study has not been performed on Zbtb20-/- mutant mice.

The expression of calbindin (CB) in developing Purkinje cells is similar in many species such as mouse (Larouche, 2006), rat (Wierzba-Bobrowicz, 2011), cat (Résibois, 2004), human (Milosevic, 1998) and chicken (Pires, 2006). Studies on the distribution of CB immunopositive (CB+) Purkinje cells in chicks at E8, E10, E12, E14, E16, E18 and E20 show that there is a dynamic and asynchronous pattern of distribution of immunopositive cells (Gilbert, 2012). By E10, clusters of CB+ cells are observed in folia II, III/IV, VII and VIII. The most intense staining is in folia VII, VIII and IX. After E14, the majority of Purkinje cells are CB+ with well-developed bodies and distinct dendritic processes. By E18, a three-layered cerebellar cortex is observed, in which the bodies of the pyriform neurons form the Purkinje layer (Gilbert, 2012).

When examining the quantity and distribution of unipolar brush cells, we found that on the fourth, eighth and twelfth postnatal days their number was similar in wild-type and mutant mice. It is likely that the lack of Zbtb20 does not affect the proliferation of unipolar brush cells in postnatal life. A review of the available literature shows that our study is the first conducted on Zbtb20-/- mutants.

Studies on the distribution of CR in the cerebellum of Cacna1a-/- mice (Cacna1- gene encoding calcium ion channels) showed weaker expression in mutants compared to controls (Kim, Niimi et al. 2016). A similar study in RyR1-/- mice (RyR1-ryanodine receptor 1) found weaker expression of CR in the cerebellar cortex in mutants compared to controls (Cicale, Ambesi-Impiombato et al. 2002). In rats without gene mutations (age P12-30 months) no difference in CR expression in the cerebellar cortex was found at different age periods (Villa, Podini et al. 1994).

In our developmental studies of Golgi type II cells, we found that at P4, P8 and P12 there were similar numbers of cells in wild-type and mutant mice, with a slight predominance in controls, and this is the first study of its kind in Zbtb20-/- mutants. Mice in which Golgi cells were selectively inactivated by viral vectors showed impaired motor coordination in complex movements, indicating their role in this cerebellar function (Watanabe et al. 1998).

Leto et al. (2009) followed the early phases of interneuron development. To this end, they examined Pax-2 expression in wild-type mice, as well as GFP fluorescence in Pax-2-GFP mice

at P2, P6 and P9. In more than 98% of cases, Pax-2-expressing cells showed morphological and neurochemical characteristics of interneurons.

When studying the quantity and distribution of proliferating neurons in the cerebellum, we found that it was similar in wild-type and mutant mice at three age periods – P4, P8 and P12. So far, this is the first similar study of Zbtb20-/- experimental animals. Study of cell proliferation in mice in the period first to twelfth postnatal week was done using the marker Ki-67 (Nkomozepi, Mazengenya et al. 2019). Expression was observed mainly in the olfactory bulb, rostral migratory stream, subventricular zone of the lateral ventricle, subgranular zone of the dentate gyrus, neocortex and cerebellum, and it decreased sharply with advancing age (Nkomozepi, Mazengenya et al. 2019). Another study found that proliferation in the human cerebellum continues long after birth; using an anti-Ki-67 antibody, proliferating cells were detected in the EGL up to the fifth month after birth.

The dynamics of cell proliferation changes throughout development. In rodents, EGL positivity increases slightly after birth and remains at this level for about a week. By P12, a gradual decrease in proliferation begins until the layer disappears (Seress, 1978). In humans, increased labeling is observed between the 24th and 28th weeks. This suggests that the first proliferative period lasts until the 28th week. The second period lasts until the 38th–40th week, when the immunopositivity index begins to decrease. The thickness of the EGL remains constant until the second postnatal month, suggesting that the reduced proliferation is due to cell migration.

The results of our studies show the same trend in both experimental groups – an increase in the number of proliferating cells at P4–P8, after which their number decreases significantly at P12. We observed a slightly lower level of Ki-67-expressing cells in mutants at all ages, but this difference compared to control animals was statistically insignificant, suggesting that Zbtb20 does not significantly affect the proliferative process in the cerebellum. In our study, the quantity and distribution of astrocytes in the developing cerebellum at P4, P8 and P12 was measured by measuring the area of GFAP+ zones in a whole section and calculating their percentage relative to the total section area. The differences between the two experimental groups were insignificant by both criteria, but at P4 the data were in favor of the controls, while at later periods, P8 and P12, the results showed a slight prevalence in mutants. It is likely that the transcription factor Zbtb20 also does not significantly affect astrocyte proliferation, especially in the early postnatal period. In the available literature no data were found for a similar study on Zbtb20-/- experimental animals.

Overexpression of Zbtb20 in vitro or in vivo stimulates astrocytogenesis, while its lack of expression suppresses it, a trend that was also observed in our study, although to a lesser extent.

Zbtb20 is thought to regulate the early stages of astrocytogenesis in the neocortex. The transcription factor is expressed in Aldh1L1-GFP+, GFAP+ or S100β+ astrocytes in the forebrain, hippocampus, gray and white matter of the spinal cord. It is also expressed in neuronal progenitor cells isolated from the spinal cord at E11.5. Zbtb20 induces astrocyte differentiation and suppresses that of neurons and oligodendrocytes in cultures of spinal cord neuronal precursors. These results suggest that Zbtb20 regulates astrocytogenesis in multiple CNS regions (Nagao et al. 2016).

Our data are consistent with those reported in the literature. By knocking out the Zbtb20 gene, we also observed a slight increase in oligodendrocyte numbers in the cerebellum using the marker Olig2+. However, it is noteworthy that we detected a selective effect on the distribution of newly formed oligodendrocytes, a finding that has not been reported before. At P12, we found a statistically significant predominance of oligodendrocytes in the third, sixth, and seventh folia, which is novel, but the significance of this phenomenon is still unknown. This question requires further investigation.

Mutation of one allele of Zbtb20 in heterozygous hAPP-J20 mice alters its expression in some brain regions but not in others. Deficits in learning, memory, behavioral abnormalities, dysfunction of neuronal networks, and changes in hippocampal neurons in Alzheimer's disease are unlikely to be caused by reduced levels of Zbtb20 (Gulbranson et al. 2021).

NeuN is considered a marker for studying neurons. In albino rats, NeuN expression has been found in migrating granule neurons from the EGL to the IGL, as well as in mature IGL neurons from P2 to P15 (Zimatkin and Karniushko, 2016). Hyperoxia in rats reduces NeuN expression by P30, compared to controls, which is associated with neuronal loss (Scheuer et al., 2018). In experimental animals with a Reelin (Reln-/-) gene mutation, expression of NeuN is observed after P5. There is no statistically significant difference between Reln-/- and controls (Reln+/+) (Cocito et al., 2016). Placing rats at P7 in conditions of increased O_2 content leads to a decrease in the number of NeuN+ cells, compared to controls exposed to normoxia, which proves the damaging effect of increased O_2 pressure on neurogenesis in the cerebellum (Scheuer, et al. 2018).

Examining the number of neurons and their distribution across folias at the three age periods (P4, P8 and P12) using this marker for postmitotic neurons, we did not find a difference in the number of cells expressing NeuN, comparing the two groups of experimental animals. Some differences were observed between the individual folias, but they were not statistically significant. It is likely that the transcription factor Zbtb20 does not have a significant effect on

postmitotic neurons in the developing cerebellum. A similar study on Zbtb20-/- experimental animals has not been conducted so far.

With our study, we demonstrate for the first time that in the postnatal period (P12) in some of the cerebellar folia (fourth, ninth and tenth) of homozygous Zbtb20-/- mutants, a greater thickness of the outer granular layer is established, compared to wild-type mice. This is probably due to a delayed migration of granule cells from the outer granular to the inner granular layer in homozygous mutants. This is found in areas where we observe additional folds of the cerebellar folia in the mutants (fourth and fifth folia).

Numerous studies have shown that there is a correlation between the development and migration of granular neurons and the growth of the cerebellum in the postnatal period. Granule neurons are also associated with the growth and additional folding of the cerebellar folds. Experimental animal models with a severely reduced number of granule cells develop abnormalities in the formation of folia and fissures in the postnatal cerebellum (Herrup K., et al. 1987). The directed proliferation of granule neurons is likely involved in determining the shape and size of the cerebellar lobes (Legué et al., 2015; 2016). The development of granule neurons is regulated by transcription factors. One of them is Atoh1, which begins its expression at E13 in the rhombic lip. In the absence of this factor, granule neurons are not generated and the outer granular layer is not formed (Van der Heijden et al., 2021).

The formation of cerebellar macrostructures depends not only on the expansion of the granule cell population, but also on their maturity. The lack of liver kinase B1 (Lkb1) leads to an increased size of the cerebellum and a greater number of foliation folds, without affecting proliferation. Slow radial migration of granule neurons is observed (Ryan et al., 2017). Another mechanism by which foliation is affected is the uneven migration of granule cells from the external granular layer to the internal granular layer and subsequent elongation of the cerebellar folds (Takeda et al., 2021). The development of the cerebellar lobes is also influenced by the chromodomain helicase DNA-binding proteins CHD7 and CHD8. Disrupted CHD7 function is associated with CHARGE syndrome, and those of CHD8 with autism spectrum disorders. Deletion of CHD8 in granule neuron precursors is associated with defects in foliation due to premature differentiation of granule neurons (Chen et al., 2022). In CHD7-/- experimental animals, a reduced number of cerebellar sheets along the anterior-posterior axis is observed (Reddy et al., 2021). Deletion of CHD7 does not alter the proliferative capacity of granule neuron precursors, as well as their migration. Only the axis of migration changes from anterior-posterior to medio-lateral. Therefore, the axis of spread of these cells is an important factor for cerebellar foliation (Legué et al., 2015; Lejeune et al., 2019).

Conclusion

The central nervous system is a complexly organized structure that functions through the interaction of millions of neurons and neuroglial cells. Of interest to modern science is the signaling and normal development of neurons and glia, as well as the molecular mechanisms that determine them. Although it is now believed that the molecular mechanisms responsible for the development of neuronal and neuroglial precursors in the cerebellum have been clarified, some mysteries remain that need to be unraveled. For example, there is still no understanding of the mechanisms that determine the development and differentiation of the nine types of Purkinje cells. Future studies that shed more light on the occurrence of congenital cerebellar malformations would be of interest to neuroscience. These conditions could cause impaired coordination, gait disturbances, and speech deficits. An important discovery is the isthmic organizer, which secretes Fgf8 and thus unlocks the molecular mechanisms for cerebellar specification.

Cerebellar neurons originate from two main neurogenic niches: the rhombic lip and the ventricular zone. Genetic analysis has established that glutamatergic neurons are neurons in the cerebellar nuclei, some of the granular neurons, and unipolar brush cells. They originate from the rhombic lip and are determined by the transcription factor ATOH1. GABAergic neurons originate from the ventricular zone and are determined by the transcription factor PTF1a. These include Purkinje cells, interneurons in the molecular layer, Golgi and Lugaro cells, and GABAergic neurons of the deep cerebellar nuclei.

The knowledge accumulated in recent years seems to refute the postulate that the cerebellum is involved only in the motor function of the organism. More and more data are accumulating about its important role in behavioral patterns. Here too, the molecular mechanisms are still unknown. Given the rapid growth of the cerebellum around birth, it is vulnerable to developmental disorders. This vulnerability is due to the extensive connections between it and the cerebral cortex. Disorders in the cerebral cortex-cerebellum circuit can lead to the emergence of psychiatric disorders in early childhood.

Our study has shed some light on the role of certain transcription factors in cerebellar development. The main focus was on the transcription factor Zbtb20. We found that it influences the folding of the cerebellar foliations during development, influences the size of the newly forming cerebellum, and influences the development of unipolar brush cells, Golgi cells, astrocytes, and oligodendrocytes. Future, more extensive studies on the issues addressed in this dissertation, as well as the inclusion of previously unexplored transcription factors regulating

cerebellar formation in humans, would contribute not only to a more complete understanding of the mechanisms of normal development, but also of those leading to pathological changes in this important part of the nervous system.

Contributions of the Dissertation

Original Contributions

1. For the first time, a quantitative analysis of Purkinje cells is performed on the cerebellum of Zbtb20$^{-/-}$ mice on the fourth, eighth and twelfth postnatal days.
2. For the first time, a quantitative analysis of unipolar brush cells is performed on the cerebellum of Zbtb20$^{-/-}$ mice on the fourth, eighth and twelfth postnatal days.
3. For the first time, a quantitative analysis of Golgi cells is performed on the cerebellum of Zbtb20$^{-/-}$ mice on the fourth, eighth and twelfth postnatal days.
4. For the first time, an analysis of the quantity and distribution of granular neurons in the cerebellum of Zbtb20$^{-/-}$ mice on the fourth, eighth and twelfth postnatal days is performed.
5. For the first time, astrocytes were analyzed in the cerebellum of Zbtb20$^{-/-}$ mice on the fourth, eighth, and twelfth postnatal days.
6. For the first time, the quantity and distribution of oligodendrocytes in the cerebellum of Zbtb20$^{-/-}$ mice were analyzed in the fourth, eighth, and twelfth postnatal days.
7. For the first time, proliferating cells were analyzed in the cerebellum of Zbtb20$^{-/-}$ mice on the fourth, eighth, and twelfth postnatal days.
8. For the first time, the area of the cerebellum was measured, as well as its individual layers – molecular, external granular, internal granular, Purkinje cell layer. The measurements were made on histological preparations of Zbtb20$^{-/-}$ mice on the fourth, eighth, and twelfth postnatal days.

Publications connected with the Dissertation

Iskren Velikov. Transcription factors in cerebellar development. Trakia Journal of Sciences, Vol.21, 2023, No.3 (257-265). doi:10.15547/tjs.2023.03.007

Participation in scientific forums in connection with the Dissertation

Velikov I.B., Stoyanova I.I., Tonchev A.B. Role of transcription factor Zbtb20 in the cerebellar morphogenesis. XXIV Congress of BAS, May 31- June 2 2019, Stara Zagora, Bulgaria

Velikov IB, Stoykova A, Tonchev AB, Stoyanova II. Role of the transcription factor Zbtb20 in the cerebellar cortex development. Black Sea symposium for Young Scientists in Biomedicine, November 22- 24 2019, Varna, Bulgaria

Velikov IB, Stoykova A, Tonchev AB, Stoyanova II.
Role of Doublecortin in the cerebellar cortex development in Zbtb20-knockout mice, XI International symposium on Clinical Anatomy, Varna, Bulgaria, 2-4 October 2020

Velikov IB, Stoykova A, Tonchev AB, Stoyanova II.
Calbindin expression in the cerebellar cortex of Zbtb20 knockout mice, XI International symposium on Clinical Anatomy Varna, Bulgaria, 2-4 October 2020

Velikov IB., Programmed cell death in Zbtb20 knockout mice. XXV National Congress of the Bulgarian Anatomical Society with international participation 28 – 30 May 2021 Pleven, Bulgaria

Velikov I.B., Stoyanova I.I., Stoykova A., Tonchev A.B., Pax2 expression in developing cerebellum of Zbtb20-/- mice. Black sea neurogenesis, Varna, Bulgaria, May 26-28 2022

Acknowledgements

I express my gratitude to my parents – Krasimira and Boyan Velikovi for their unconditional support during these six years of work on my Dissertation.

I express my gratitude to my scientific supervisor – Professor Dr. Irina Stoyanova – van der Laan for her support, guidance and valuable advice during my studies in the Phd program.

I express my gratitude to Professor Dr. Anastasia Stoykova for the provided histological preparations.

I express my gratitude to Professor Dr. Anton Tonchev for the methodological guidance during our twelve years of shared work.

I express my gratitude to the Head of the Department of Anatomy and Cell Biology – Associate Professor Dr. Stoyan Pavlov for the guidance on technical issues that he gave me.

I express my gratitude to Dr. Dimo Stoyanov, MD and Dr. Lora Veleva for their support in preparing some of the histological preparations and photographing them.

I express my gratitude to the laboratory assistants Velina Kenovska, Yordanka Yaneva, Svetla Kostadinova and Elena Boeva † for their technical support in the preparation of the histological preparations.

I express my gratitude to the team of the Max Plank Institute in Göttingen (Germany), who contributed to the breeding of Zbtb20$^{-/-}$ transgenic mice and wild-type mice at the ages of P4, P8 and P12.